

On a discrete scheme for the Mullins-Sekerka flow and its fine properties

Tokuhiro Eto*

March 1, 2022

Abstract

The Mullins-Sekerka problem is numerically solved in \mathbb{R}^2 with the aid of the charge simulation method. This is an expansion of a numerical scheme by which Sakakibara and Yazaki computed the Hele-Shaw flow. We investigate a sufficient condition for the number of collocation points to ensure that the length of generated approximate polygonal curves exactly decrease step by step. Moreover, changing fundamental solutions of the charge simulation method, we are successful to establish a numerical scheme which can be used to treat the Mullins-Sekerka problem with the right contact angle condition.

1 Introduction

The Mullins-Sekerka problem is the quasi-stationary Stefan problem with surface tension. Its solution describes the time evolution of the interface which separates two-phases that are filled by different materials. At a time t , one material is filled in a bounded smooth region Ω_t and another material is filled in the outer region $\mathbb{R}^2 \setminus \overline{\Omega_t}$. The boundary $\Gamma_t = \partial\Omega_t$ implies the interface. The temperature of the material is denoted by $u = u(t, x)$ for $x \in \mathbb{R}^2 \setminus \Gamma_t$ and $t \geq 0$. Then, the Mullins-Sekerka problem asks us to find (u, Γ_t) satisfying

$$\begin{cases} \Delta u = 0 & \text{in } \mathbb{R}^2 \setminus \Gamma_t, \\ u = \kappa & \text{on } \Gamma_t, \\ \nabla u(x) = O\left(\frac{1}{|x|^2}\right) & \text{as } |x| \rightarrow \infty, \\ V = -\left[\frac{\partial u}{\partial \mathbf{n}}\right] & \text{on } \Gamma_t, \end{cases} \quad (1)$$

where \mathbf{n} denotes the normal vector to Γ_t outgoing from Ω_t and κ designs the curvature of Γ_t . The normal velocity of Γ_t is denoted by V . To be more precise, the motion of Γ_t is governed by

$$\frac{d}{dt} \mathbf{X}(t, s) = V(t, \mathbf{X}(t, s)) \mathbf{n}(t, \mathbf{X}(t, s)) \quad (t \geq 0, s \in [0, 2\pi]), \quad (2)$$

where the interface Γ_t is parameterized as $\mathbf{X}(t, s)$ for $s \in [0, 2\pi]$. V describes the speed of Γ_t in the direction to \mathbf{n} . Let $[\varphi]$ be the jump in the normal direction of a quantity φ across Γ , namely, $[\varphi](x) := \lim_{\varepsilon \rightarrow 0} \{\varphi(x - \varepsilon \mathbf{n}) - \varphi(x + \varepsilon \mathbf{n})\}$ for each $x \in \Gamma_t$.

*Email-address: tokuhiro_eto@yahoo.co.jp

The Mullins-Sekerka equation is a limit of phase field model, which is so called the Cahn-Hilliard equation where two phases are separated by a transition layer instead of a shape interface. The Cahn-Hilliard equation is important to understand the Spinodal decomposition which explains a phenomenon that compounded solutes and solids are stable with high temperature but become unstable with low temperature and eventually separated by sharp interfaces. The convergence of the Cahn-Hilliard equation to the Mullins-Sekerka equation was first shown by Pego [17] in a formal manner. Stoth [21] gave a rigorous proof of the convergence in the case where a domain under consideration is a ball in \mathbb{R}^3 and an initial data and boundary values are all radially symmetric. In a general dimension, Alikakos et al. [2] proved that a family of smooth solutions to the Cahn-Hilliard equation tends to a smooth solution to the Mullins-Sekerka equation provided that the latter exists.

The Mullins-Sekerka problem has been well studied in the analytical point of view. Chen et al. [6] proved the existence of a classical solution to the Mullins-Sekerka problem local in time in the two dimensional case, so did Escher and Simonett [8] in general dimensional cases. In the literature of weak solutions, Luckhaus and Sturzenhecker [13] proposed a weak notion of solution to the Mullins-Sekerka problem and gave its global time existence result whenever the sum of the surface area measure does not change discontinuously in time. As indicated in our experiment, this setting cannot be applied in the case where multi particles exist and they are very close each other. (See Section 4.6.) Röger [19] was successful to remove this assumption in terms of geometric measure theory.

There are several works that treated the Hele-Shaw problem or the Mullins-Sekerka problem numerically. Though the typical Mullins-Sekerka problem is considered in a bounded domain with smooth boundary, Bates et al. [4] considered the problem (1) in \mathbb{R}^2 and translated the original problem (1) into a corresponding boundary integral equation. Eventually, they did not have to care about the boundary of the container. Then, they split an initial curve into several segments and regarded as a part of circles. In this way, they could calculate a discrete version of the curvatures and derive a linear system of equations whose unknown variables are normal velocities at each vertex by means of the Gibbs-Thomson law. (This is the second condition of (1).) Recall that our unknown variables on the linear system are coefficients of fundamental solutions in contrast to their scheme. (See (10) and (12).) Moreover, they adopted the semi implicit method when they solved the linear system to make their scheme stable with a small time step. For other studies using the boundary integral method, we refer the reader to [22], [15] and [5]. Barrett et al. [3] proposed a parametric finite element scheme for the Stefan problem with surface tension and proved the well-posedness and stability of their scheme. In the course of the discussion, they also revealed that the scheme is applicable for the Mullins-Sekerka problem. Feng and Prohl [9] showed that their numerical scheme, so called the fully discrete mixed finite element scheme, to construct discrete solutions to the Cahn-Hilliard equation tends to the solution of the Mullins-Sekerka equation provided that a global-in-time classical solution to it exists.

The purpose of this paper is to propose a discrete scheme to solve the Mullins-Sekerka problem numerically and to reveal that our scheme has some fine properties. To this end, we followed the scheme proposed by Sakakibara and Yazaki [20]. Moreover, we confirm that the proposed scheme possesses a curve shortening property, CS for short, and an area preserving property, AP for short. These facts are predictable since the original scheme for the Hele-

Shaw problem also has the property. However, we focus on CS and derive a discrete variant of estimation related to the length of the curve. This outcome is reported in Corollary 1.

At this stage, let us give a brief explanation of our scheme. Suppose that a smooth curve Γ_t is given for some $t > 0$. Then, Γ_t is approximated by an N polygon Γ_t^N where $N \geq 3$ is a positive integer. The interior domain of Γ_t^N is designated as Ω_t^N . The vertices of Γ_t^N are denoted by $\mathbf{X}_i (1 \leq i \leq N)$. For convenience, we adopt a periodic rule to indexes of \mathbf{X}_i 's like $\mathbf{X}_0 = \mathbf{X}_N$ and $\mathbf{X}_{N+1} = \mathbf{X}_1$. Each edge $[\mathbf{X}_{i-1}, \mathbf{X}_i]$ is expected to possess discrete version of curvatures $\kappa_i = \kappa_i(t) (1 \leq i \leq N)$. Additionally, normal vectors $\mathbf{N}_i = \mathbf{N}_i(t)$ and tangential vectors $\mathbf{T}_i = \mathbf{T}_i(t)$ at \mathbf{X}_i are suitably defined. Among standard numerical methods, we adopt the charge simulation method, written as CSM for short, that was originally developed to approximate a solution to the Laplace equation in a bounded domain with Dirichlet boundary condition. CSM is a variant of the method of fundamental solutions, written as MFS for short, in which approximate solutions are expressed in the form of a linear combination of fundamental solutions to partial differential equations under consideration. CSM asks one to choose proper charge points y_1^+, \dots, y_N^+ from $\mathbb{R}^2 \setminus \Omega_t^N$ and collocation points $\mathbf{X}_1, \dots, \mathbf{X}_N$ on Γ_t and express an approximate solution as follows.

$$U^+(x) = \sum_{i=1}^N Q_i^+ E(x - y_i^+) \quad (3)$$

where E is the fundamental solution of the Laplace equation, that is $E(x) := \frac{1}{2\pi} \log|x|$ for $x \in \mathbb{R}^2 \setminus \{0\}$. Since y_i^+ 's are outside of Ω^N , U^+ is harmonic at all points in Ω^N . The coefficients Q_i 's should be determined by Dirichlet boundary conditions $U(\mathbf{X}_i) = \kappa(\mathbf{X}_i)$ for $1 \leq i \leq N$. This is the basic idea of CSM. For more detail about CMS, see Katsurada and Okamoto [12]. The above conventional scheme was modified by Murota [16] to make the scheme possess invariance properties that original continuous problems also have. Concretely, he alternatively used the following combination.

$$U^+(x) = Q_0^+ + \sum_{i=1}^N Q_i^+ E(x - y_i^+).$$

In this scheme, we have to add an equality to a linear system because we have one more value Q_0^+ to find. For instance, Murota assumed that the sum of Q_i^+ 's equals zero. In solving the Hele-Shaw problem numerically, Sakakibara and Yazaki [20] improved Murota's invariant scheme to make this additional assumption much more natural. They defined dummy singular points $z_i^+ (1 \leq i \leq N)$ and replaced combination of fundamental solutions by

$$U^+(x) = Q_0^+ + \sum_{i=1}^N Q_i^+ \{E(x - y_i^+) - E(x - z_i^+)\}. \quad (4)$$

It can be observed that the above function U^+ is invariant under translation and scaling without any additional assumption. Hence, it is possible to impose an area preserving requirement that seems to be more natural one than the zero average assumption. Taking singular points y_i^- and z_i^- from Ω_t^N , we also have a function U^- being harmonic in $\mathbb{R}^2 \setminus \Omega_t^N$ that satisfies the Dirichlet boundary condition boundary. To find such a U^- , we should solve an external potential problem, although it is not possible by neither the finite difference method nor the

finite element method because of the unboundedness of the domain where the problem is considered. As imposed in the fourth equality of (1), each point x on Γ_t^N is required to move at the speed that equals the jump of the normal derivatives of U^+ and U^- across Γ_t^N . Once we obtain such U^+ and U^- , a direct differentiation of U^+ and U^- yields the representative normal velocity $V_i(t) = V_i^+(t) + V_i^-(t)$ at \mathbf{X}_i . Consequently, \mathbf{X}_i should fulfill the evolution equation

$$\frac{d}{dt}\mathbf{X}_i(t) = V_i(t)\mathbf{N}_i(t) + W_i(t)\mathbf{T}_i(t) \quad \text{for } 1 \leq i \leq N, t > 0. \quad (5)$$

Tangential velocity W_i and its vector \mathbf{T}_i is needed to make the scheme stable although they have no effect on the geometry of a curve. (See Proposition 2.4 [7] for instance.) Normal velocity V_i and its vector \mathbf{N}_i definitely control the motion of a curve. Finally, we discretize the time variable as $t = n\Delta t$ ($0 \leq n \leq N$) and rearrange the evolution equation (5) as follows.

$$\mathbf{X}_i^{n+1} = \mathbf{X}_i^n + \Delta t(V_i(t_n)\mathbf{N}_i(t_n) + W_i(t_n)\mathbf{T}_i(t_n)) \quad \text{for } 1 \leq i \leq N, n = 0, 1, \dots \quad (6)$$

A particular novelty of this paper is treating a boundary contact case of the Mullins-Sekerka problem in the half plane \mathbb{R}_+^2 . To this end, we replace the fundamental solutions of combination by the Green function on \mathbb{R}_+^2 . Since curves under consideration are open, we modify the structure of our scheme. Well-posedness of the Mullins-Sekerka problem with ninety contact angle condition was established by Abels et al. [1].

The rest of the paper is organized as follows. In Section 2, we rigorously state how to implement the proposed scheme. Section 3 is devoted to list our main results without their proofs. In Section 4, we give several examples of implementation of the scheme. Moreover, accuracy of our scheme is confirmed in terms of an annulus like domain as an initial data. We shall extend the scheme to the boundary contact cases in Section 5. In section 7, we collect all proofs of Theorems and Propositions whose justification has been postponed.

2 Numerical scheme

In this section, we present a concrete procedure to construct approximate polygons. This is a natural extension of the scheme proposed in [20].

2.1 Polygonal approximation of the interface

Let $N \geq 3$ be a positive number and Ω^N be an N polygonal domain in \mathbb{R}^2 having vertices $\mathbf{X}_1, \dots, \mathbf{X}_N \in \mathbb{R}^2$. Set $\mathbf{X}_0 := \mathbf{X}_N, \mathbf{X}_{N+1} := \mathbf{X}_1$. This periodic rule is always applied unless otherwise stated explicitly. The symbol $[\mathbf{X}_{i-1}, \mathbf{X}_i]$ denotes the line segment connecting \mathbf{X}_{i-1} and \mathbf{X}_i . This is called the edge in the sequel. Then, the boundary $\Gamma^N := \partial\Omega^N$ readily designs an N polygon and expressed as $\Gamma^N = \cup_{i=1}^N [\mathbf{X}_{i-1}, \mathbf{X}_i]$. For each $1 \leq i \leq N$, define

$$r_i := |\mathbf{X}_i - \mathbf{X}_{i-1}|, \quad \mathbf{t}_i := \frac{\mathbf{X}_i - \mathbf{X}_{i-1}}{r_i}, \quad \mathbf{n}_i := \mathbf{t}_i^\perp. \quad (7)$$

Here we have use the notation $(a, b)^\perp := (b, -a)$. Moreover, the midpoint of the edge $[\mathbf{X}_{i-1}, \mathbf{X}_i]$ is denoted by \mathbf{X}_i^* , namely $\mathbf{X}_i^* := \frac{\mathbf{X}_{i-1} + \mathbf{X}_i}{2}$. The outer angle φ_i of Γ^N at each vertex \mathbf{X}_i is written by

$$\varphi_i := \text{sgn}(\mathbf{t}_i, \mathbf{t}_{i+1}) \arccos(\mathbf{t}_i \cdot \mathbf{t}_{i+1}).$$

where the function sgn is defined by

$$\text{sgn}(\mathbf{a}, \mathbf{b}) := \begin{cases} 1 & \text{if } \mathbf{a} \cdot \mathbf{b}^\perp > 0, \\ 0 & \text{if } \mathbf{a} \cdot \mathbf{b}^\perp = 0, \\ -1 & \text{otherwise.} \end{cases}$$

for each $\mathbf{a}, \mathbf{b} \in \mathbb{R}^2$. Using φ_i , we set

$$\cos_i := \cos\left(\frac{\varphi_i}{2}\right), \quad \sin_i := \sin\left(\frac{\varphi_i}{2}\right), \quad \tan_i := \frac{\sin_i}{\cos_i}.$$

Then, we define a discrete curvature of Γ^N at \mathbf{X}_i^* as follows.

$$\kappa_i := \frac{\tan_i + \tan_{i-1}}{r_i} \quad \text{for } i = 1, \dots, N. \quad (8)$$

Moreover, let us define a normal vector \mathbf{N}_i and a tangential vector \mathbf{T}_i at \mathbf{X}_i in terms of the normal vector \mathbf{n}_i and the tangential vector \mathbf{t}_i of the edge $[\mathbf{X}_{i-1}, \mathbf{X}_i]$ as follows.

$$\mathbf{N}_i := \frac{\mathbf{n}_i + \mathbf{n}_{i+1}}{2 \cos_i}, \quad \mathbf{T}_i := \frac{\mathbf{t}_i + \mathbf{t}_{i+1}}{2 \cos_i} \quad \text{for } i = 1, \dots, N.$$

2.2 Approximation of the normal velocity

Solve the internal problem. In this step, we solve the Laplace equation with a Dirichlet boundary condition which is given by κ_i . To this end, we must choose singular points y_1^+, \dots, y_N^+ and dummy singular points z_1^+, \dots, z_N^+ from $\mathbb{R}^2 \setminus \bar{\Omega}$. For small $d > 0$, we set

$$y_i^+ := \mathbf{X}_i^* + d\mathbf{n}_i, \quad z_i^+ := \mathbf{X}_i^* + \frac{d}{2}\mathbf{n}_i.$$

Then, suppose that the solution of the Dirichlet boundary problem is of the form

$$U^+(x) = Q_0^+ + \sum_{i=1}^N Q_i^+ \{E(x - y_i^+) - E(x - z_i^+)\} \quad (9)$$

for some $Q_0^+, Q_1^+, \dots, Q_N^+ \in \mathbb{R}$. U^+ is clearly harmonic in Ω^N due to its structure. To determine these values, we shall solve the following linear system of equations.

$$\begin{cases} Q_0^+ + \sum_{j=1}^N Q_j^+ \mathbb{G}_{i,j} = \kappa_i & \text{for } i = 1, \dots, N, \\ \sum_{j=1}^N Q_j^+ H_j = 0. \end{cases} \quad (10)$$

where

$$\begin{aligned} \mathbb{G}_{i,j} &:= E(\mathbf{X}_i^* - y_j) - E(\mathbf{X}_i^* - z_j), \\ H_j &:= -\sum_{i=1}^N \mathbf{H}_{i,j} \cdot \mathbf{n}_i r_i, \\ \mathbf{H}_{i,j} &:= \nabla E(\mathbf{X}_i^* - y_j^+) - \nabla E(\mathbf{X}_i^* - z_j^+). \end{aligned}$$

Solve the external problem. Similarly as the previous step, take singular points y_1^-, \dots, y_N^- and dummy singular points z_1^-, \dots, z_N^- in Ω^N as follows.

$$y_j^- := \mathbf{X}_i^* - d\mathbf{n}_i, \quad z_j^- := \mathbf{X}_i^* - \frac{d}{2}\mathbf{n}_i.$$

Then, the solution of the exterior Dirichlet boundary problem is written by

$$U^-(x) = Q_0^- + \sum_{i=1}^N Q_i^- \{E(x - y_i^-) - E(x - z_i^-)\} \quad (11)$$

where $Q_0^-, Q_1^-, \dots, Q_N^-$ are selected to fulfill

$$\begin{cases} Q_0^- + \sum_{j=1}^N Q_j^- G_{i,j} = \kappa_i & \text{for } i = 1, \dots, N, \\ -\sum_{j=1}^N Q_j^- H_j = 0. \end{cases} \quad (12)$$

Derive the normal velocity. Once Q_i^+ and Q_i^- are determined, we can define a representative normal velocity at \mathbf{X}_i . Setting $v_i^+ := -\nabla U^+(\mathbf{X}_i^*) \cdot \mathbf{n}_j$ and $v_i^- := -\nabla U^-(\mathbf{X}_i^*) \cdot (-\mathbf{n}_i)$, we define representative normal velocities by

$$V_i^\pm := \frac{v_i^\pm + v_{i+1}^\pm}{2 \cos_i} \quad \text{for } i = 1, \dots, N. \quad (13)$$

Derive the tangential velocity. To reduce instability of the scheme, we are forced to consider a tangential vector which does not affect the shape of the polygon. To this end, we adopt a uniformly distribute method, UDM for short. Let us only state formulae to obtain tangential velocities. We refer the reader to Sakakibara and Yazaki [20] for derivation of the scheme.

Tangential velocities $W_i (1 \leq i \leq N)$ are defined by

$$W_i := \frac{\Psi_i + C}{\cos_i} \quad \text{for } 1 \leq i \leq N, \quad C := -\frac{\sum_{i=1}^N \frac{\Psi_i}{\cos_i}}{\sum_{i=1}^N \frac{1}{\cos_i}}. \quad (14)$$

Here we have set $\Psi_i := \sum_{j=1}^i \psi_j$ for each $1 \leq i \leq N$ where $\psi_1 := 0$ and

$$\psi_i := \frac{1}{N} \sum_{i=1}^N \kappa_i (v_i^+ + v_i^-) r_i - (V_i^+ + V_i^-) \sin_i - (V_{i-1}^+ + V_{i-1}^-) \sin_{i-1} + \left(\frac{L}{N} - r_i \right) \omega$$

for $2 \leq i \leq N$ with $L := \sum_{i=1}^N r_i$ and $\omega := 10N$.

2.3 Time evolution of the polygonal interface

We are now in the position to state our numerical scheme. Given an initial curve $\Gamma_0 = \partial\Omega_0$, we approximate it by an N polygonal curve

$$\Gamma_0^N = \bigcup_{i=1}^N [\mathbf{X}_{i-1}^{(0)}, \mathbf{X}_i^{(0)}]$$

where $\mathbf{X}_i^{(0)}$ ($1 \leq i \leq N$) denote vertices of Γ_0^N . The domain surrounded by Γ_0^N is written by Ω_0^N . For $t > 0$, suppose that an N polygon Γ_t^N is an approximation of Γ_t to be found. The vertices of Γ_t^N are denoted by $\mathbf{X}_i = \mathbf{X}_i(t)$ ($1 \leq i \leq N$). Quantities $\kappa_i = \kappa_i(t)$, $\mathbf{N}_i = \mathbf{N}_i(t)$, $\mathbf{T}_i = \mathbf{T}_i(t)$, $V_i^+ = V_i^+(t)$, $V_i^- = V_i^-(t)$, $V_i = V_i(t) := V_i^+ + V_i^-$ and $W_i = W_i(t)$ are defined as above. Following the continuous version of evolution law, we consider

$$\frac{d}{dt}\mathbf{X}_i(t) = V_i(t)\mathbf{N}_i(t) + W_i(t)\mathbf{T}_i(t) \quad \text{for } i = 1, \dots, N, \quad t > 0 \quad (15)$$

with the initial condition $\mathbf{X}_i(0) = \mathbf{X}_i^{(0)}$ ($1 \leq i \leq N$). Finally, the time variable is discretized as $t_n = n\Delta t$ ($n = 0, 1, \dots$) with a given time step $\Delta t > 0$ and the forward Euler method is applied to (15). Using the notations $\mathbf{X}_i^n = \mathbf{X}_i(t_n)$, $V_i^n = V_i(t_n)$, $\mathbf{N}_i^n = \mathbf{N}_i(t_n)$, $W_i^n = W_i(t_n)$ and $\mathbf{T}_i^n = \mathbf{T}_i(t_n)$, we provide the fully discrete scheme below.

$$\mathbf{X}_i^{n+1} = \mathbf{X}_i^n + \Delta t(V_i^n\mathbf{N}_i^n + W_i^n\mathbf{T}_i^n) \quad \text{for } i = 1, \dots, N, \quad n = 0, 1, \dots \quad (16)$$

with the initial condition $\mathbf{X}_i^0 = \mathbf{X}_i^{(0)}$ ($1 \leq i \leq N$). An N polygonal curve which consists of the vertices \mathbf{X}_i^n ($1 \leq i \leq N$) solving (16) is designated as $\Gamma_{\Delta t}^{N,n}$. The interior domain of $\Gamma_{\Delta t}^{N,n}$ is denoted by $\Omega_{\Delta t}^{N,n}$.

3 Properties of the scheme

As mentioned in Introduction, the proposed numerical scheme is expected to have the area preserving property and the curve shortening property since the original continuous problem has such properties. At this time, we assume that Γ_t is a simply closed curve that separates \mathbb{R}^2 into a bounded domain Ω_t and an unbounded domain $\mathbb{R}^2 \setminus \overline{\Omega}_t$. Suppose that (u, Γ_t) is a solution of the Mullins-Sekerka problem (1). Let us distinguish u inside of Ω_t by writing u^i , while u outside of Ω_t is presented as u^e . Then, the area \mathfrak{A}_t of Ω_t never changes. Indeed, we compute

$$\begin{aligned} \frac{d}{dt}\mathfrak{A}_t &= \int_{\Gamma_t} V dS = - \int_{\Gamma_t} \left[\frac{\partial u}{\partial \mathbf{n}} \right] dS = \int_{\Gamma_t} \left(\frac{\partial u^e}{\partial \mathbf{n}} - \frac{\partial u^i}{\partial \mathbf{n}} \right) dS \\ &= - \int_{B(0,R) \setminus \overline{\Omega}_t} \Delta u^e dx + \int_{\partial B(0,R)} \frac{\partial u^e}{\partial \mathbf{n}} dS - \int_{\Omega_t} \Delta u^i dx \\ &= 2\pi R \cdot O\left(\frac{1}{R^2}\right) \quad \text{as } R \rightarrow \infty. \end{aligned}$$

Here $R > 0$ is arbitrarily taken so large that $\Omega_t \subset\subset B(0, R)$. Thus, $\frac{d}{dt}\mathfrak{A}_t = 0$. Moreover, we see that the length \mathfrak{L}_t of Γ_t is not increasing in time. Indeed,

$$\begin{aligned} \frac{d}{dt}\mathfrak{L}_t &= \int_{\Gamma_t} \kappa V dS = - \int_{\Gamma_t} u \left[\frac{\partial u}{\partial \mathbf{n}} \right] dS = \int_{\Gamma_t} \left(u \frac{\partial u^e}{\partial \mathbf{n}} - u \frac{\partial u^i}{\partial \mathbf{n}} \right) dS \\ &= - \int_{B(0,R)} |\nabla u|^2 dx + \int_{\partial B(0,R)} u \frac{\partial u^e}{\partial \mathbf{n}} dS - \int_{B(0,R) \setminus \overline{\Omega}_t} u^e \Delta u^e dx - \int_{\Omega_t} u^i \Delta u^i dx. \end{aligned}$$

Since $\nabla u = O\left(\frac{1}{|x|^2}\right)$ as $|x| \rightarrow \infty$, u is bounded in \mathbb{R}^2 . (See Lemma 3.) Therefore, letting $R \rightarrow \infty$, we see that the right hand side of the above identity is not positive. In this section,

we tend to observe that these fine properties are valid even in the discrete version of the solutions derived by MFS. Let us prepare several useful formulae to proceed argument. All proofs of the following results are postponed and stated in Section 7.

Let $L = L(t)$ and $A = A(t)$ be the length and the area of a polygon evolving in time being subject to (15), respectively. Namely,

$$L := \sum_{i=1}^N |\mathbf{X}_i - \mathbf{X}_{i-1}|, \quad (17)$$

$$A := \frac{1}{2} \sum_{i=1}^N \mathbf{X}_{i-1}^\perp \cdot \mathbf{X}_i. \quad (18)$$

The following formulae are used to derive tangential velocities of each vertex of the polygon.

Proposition 1. *Let L and A be defined by (17) and (18), respectively. Then, the following formulae are valid.*

$$\dot{L} = \sum_{i=1}^N \kappa_i (v_i^+ + v_i^-) r_i, \quad (19)$$

$$\dot{A} = \sum_{i=1}^N (v_i^+ + v_i^-) r_i + \text{err } A \quad (20)$$

where

$$\text{err } A := \sum_{i=1}^N \left(W_i \sin_i - \frac{v_{i+1}^+ - v_i^+}{2} - \frac{v_{i+1}^- - v_i^-}{2} \right) \frac{r_{i+1} - r_i}{2}.$$

Proposition 2 (Uniform boundedness of charges). *Set*

$$\mathbb{A}_N := \begin{pmatrix} 0 & \mathbf{H}^T \\ \mathbf{1} & \mathbb{G} \end{pmatrix}, \mathbf{Q}_N := \begin{pmatrix} Q_0 \\ Q_1 \\ \vdots \\ Q_N \end{pmatrix}, \mathbf{K}_N := \begin{pmatrix} 0 \\ \kappa_1 \\ \vdots \\ \kappa_N \end{pmatrix}.$$

where $\mathbf{H} := (H_1, \dots, H_N)^T$ and $\mathbb{G} := (G_{i,j})$. Then, the values $\sup_{N \in \mathbb{N}} \frac{1}{N} \|\mathbb{A}_N^{-1}\|_1$, $\sup_{N \in \mathbb{N}} \frac{1}{N} \|\mathbf{Q}_N\|_1$, $\sup_{N \in \mathbb{N}} \frac{1}{N} \|\mathbf{K}_N\|_1$ are finite whenever \mathbb{A}_N is regular for sufficiently large N . Especially, each charge Q_i ($0 \leq i \leq N$) has the order $O(1)$.

Theorem 1 (Curve shortening property). *Assume that L is defined by (17). Then, it holds that*

$$\dot{L} \leq - \int_{\Omega_t^N} |\nabla U^+|^2 - \int_{B_R \setminus \overline{\Omega_t^N}} |\nabla U^-|^2 + O(N^2 \log N) + C_N \cdot O\left(\frac{1}{R}\right) \quad \text{as } N, R \rightarrow \infty \quad (21)$$

where C_N denotes a positive constant depending on N .

Remark 1. In spite of the term $O(N^2 \log N)$, the right hand side of (21) becomes non-positive for N large enough. Indeed, since $d \leq |x - y_j| \leq d + \text{diam}(\Omega^N)$ for each $1 \leq j \leq N$ and $x \in \overline{\Omega^N}$, it holds that $|x - y_j| = O(\frac{1}{\sqrt{N}})$. A similar argument to Lemma 1 (See Section 7.) shows

$$\left(\frac{x - y_j}{|x - y_j|^2} - \frac{x - z_j}{|x - z_j|^2} \right) = O(\sqrt{N}).$$

Hence a direct calculation gives

$$\begin{aligned} |\nabla U^+(x)|^2 &= \frac{1}{4\pi^2} \sum_{j=1}^N Q_j^+ \left(\frac{x - y_j}{|x - y_j|^2} - \frac{x - z_j}{|x - z_j|^2} \right) \cdot \sum_{j=1}^N Q_j^+ \left(\frac{x - y_j}{|x - y_j|^2} - \frac{x - z_j}{|x - z_j|^2} \right) \\ &= \sum_{i,j=1}^N O(1) \times O(1) \times O(\sqrt{N}) \times O(\sqrt{N}) = O(N^3). \end{aligned}$$

Here we have recalled that $Q_j^+ = O(1)$ for each $1 \leq j \leq N$ from Proposition 2. To get a desired property, we fix N so large that $-\int_{\Omega^N} |\nabla U^+|^2 + O(N^2 \log N)$ is negative and then send R to infinity. Note that the term $-\int_{B_R \setminus \overline{\Omega^N}} |\nabla U^-|^2$ is decreasing with respect to R . Thanks to Proposition 1, we can expect that our scheme decreases the length of the polygon step by step. This expectation turns out to be true subsequently. (See Corollary 1.)

Remark 2. If the domain which we approximate by a polygon is a circle, then the term $O(N^2 \log N)$ appearing in Theorem 1 is expected to be replaced by $O(\frac{\alpha^N}{N})$ for some $0 < \alpha < 1$. Let us write approximate solutions of (9) and (11) as $U_{(N)}^+$ and $U_{(N)}^-$, respectively. Moreover, we replace the domain on which we solve the external problem by an annulus one. Then, we can expect from the results of Katsurada (Theorem 2.2 and Theorem 4.1 [11]) and Murota (Theorem 2.4 [16]) that $U_{(N)}^+$ and $U_{(N)}^-$ exponentially converge to exact solutions U^+ and U^- as $N \rightarrow \infty$. We cannot apply these results directly because their selection for collocation points is slightly different from ours. Thus, let us assume that the results are available for our study. Since Γ^N is a regular polygon, we see that $\kappa_i = \kappa$ for every $1 \leq i \leq N$. Then, the AP property, that is the second constraints of (10) and (12), guarantees

$$\sum_{i=1}^N \int_{\Gamma_i^N} S_i(\mathbf{X}_i^*) dS = 0.$$

Since $U_{(N)}^+$ and $U_{(N)}^-$ are radially symmetric by their construction, $\nabla U_{(N)}^+ \cdot \mathbf{n}_i - \nabla U_{(N)}^- \cdot \mathbf{n}_i$ has the same sign for all $1 \leq i \leq N$. Hence we can assume that this value is non-negative without loss of generality. Then, we can estimate as follows.

$$\begin{aligned} \left| \sum_{i=1}^N \int_{\Gamma_i^N} S_i(x) dS \right| &= \left| \sum_{i=1}^N \int_{\Gamma_i} \left(U_{(N)}^+ \nabla U_{(N)}^+ \cdot \mathbf{n}_i - U_{(N)}^- \nabla U_{(N)}^- \cdot \mathbf{n}_i \right) dS \right| \\ &\leq \sum_{i=1}^N \sup_{\Gamma_i^N} |U_{(N)}^+ - U_{(N)}^-| \int_{\Gamma_i} \left(\nabla U_{(N)}^+ \cdot \mathbf{n}_i - \nabla U_{(N)}^- \cdot \mathbf{n}_i \right) dS \\ &\leq \sup_{\Omega} |U_{(N)}^+ - U_{(N)}^-| \sum_{i=1}^N \int_{\Gamma_i} \left(\nabla U_{(N)}^+ \cdot \mathbf{n}_i - \nabla U_{(N)}^- \cdot \mathbf{n}_i \right) dS. \end{aligned}$$

Here, we note that $\Gamma_i^N \subset \bar{\Omega}$ for each $1 \leq i \leq N$ to derive the last inequality. Moreover, there are no singular points and dummy singular points in the domain Ω_i^N sandwiched between Γ_i^N and $\partial\Omega$ for every $1 \leq i \leq N$ for $N \in \mathbb{N}$ large enough. To see this, recall that $|\mathbf{X}_i^* - y_i^\pm| = |\mathbf{X}_i^* - z_i^\pm| = O(\frac{1}{\sqrt{N}})$ and the width of Ω_i^N in the direction \mathbf{n}_i equals $r(1 - \cos \frac{\pi}{2N}) = O(\frac{1}{N^2})$. This clearly implies that $y_i^\pm, z_i^\pm \notin \Omega_i^N$ for sufficiently large $N \in \mathbb{N}$. Hence we obtain

$$0 = \int_{\Omega_i^N} \Delta U_{(N)}^\pm dx = \int_{\partial\Omega_i^N \cap \partial\Omega} \nabla U_{(N)}^\pm \cdot \mathbf{n} dS - \int_{\Gamma_i^N} \nabla U_{(N)}^\pm \cdot \mathbf{n}_i dS.$$

From this observation, we can proceed to calculate as follows.

$$\begin{aligned} \left| \sum_{i=1}^N \int_{\Gamma_i^N} S_i(x) dS \right| &\leq \sup_{\Omega} |U_{(N)}^+ - U_{(N)}^-| \sum_{i=1}^N \int_{\partial\Omega_i^N \cap \partial\Omega} (\nabla U_{(N)}^+ \cdot \mathbf{n}_i - \nabla U_{(N)}^- \cdot \mathbf{n}_i) dS \\ &\leq C\tau^N \int_{\partial\Omega} (\nabla U_{(N)}^+ \cdot \mathbf{n}_i - \nabla U_{(N)}^- \cdot \mathbf{n}_i) dS = O(1)\tau^N \quad \text{as } N \rightarrow \infty. \end{aligned}$$

Admitting Katsurada's result (See Remark 4.1 [11]), the integration of the right hand side of the above inequality tends to $\int_{\partial\Omega} [\frac{\partial U}{\partial \mathbf{n}}] dS$ as $N \rightarrow \infty$ and this quantity equals zero if U^+ and U^- are exact solutions to (1), respectively. In this way, we can predict that it is not necessary to take N so large to ensure the CS property holds.

Theorem 2 (Area preserving property). *Assume that the vertices \mathbf{X}_i are uniformly distributed, namely $r_i = r_{i+1}$ for each $1 \leq i \leq N$ and these are differentiable with respect to the time variable. Then, the area A surrounded by Γ is theoretically preserved for all t , that is $\dot{A} = 0$ provided that we adopt UDM.*

Theorem 1 tells us that our scheme has the CS property in some sense once we assume the differentiability of \mathbf{X}_i with respect to the time variable. Our next trial is to derive a time discrete version of Theorem 1. For simplicity of notation, let us use the symbol v_i^n in place of $v_i^+ + v_i^-$. Moreover, let r_i^n and κ_i^n denote the corresponding values of $\Gamma_{\Delta t}^{N,n}$ defined in (7) and (8), respectively.

Theorem 3 (Discrete version of CS property). *For each $n \geq 0$, let $L^n := \sum_{i=1}^N |\mathbf{X}_i^n - \mathbf{X}_{i-1}^n|$ where $\mathbf{X}_i^n (1 \leq i \leq N)$ are defined in terms of (16). Then, it holds that for each $n \geq 0$,*

$$L^{n+1} - L^n = \Delta t \sum_{j=1}^N \kappa_j^n v_j^n r_j^n + \Delta t^2 \left(O\left(\frac{1}{N}\right) \left(\sum_{j=1}^N \kappa_j^n v_j^n r_j^n \right)^2 + O(N^{\frac{3}{2}}) \sum_{j=1}^N \kappa_j^n v_j^n r_j^n + O(N^4) \right). \quad (22)$$

We deduce from Theorem 1 and Theorem 3, the highest degree with respect to N of negative terms of the right hand side of (22) equals $\max\{3 - \alpha, \frac{9}{2} - 2\alpha\}$. On the other hand, the one of positive terms equals $5 - 2\alpha$. Thus, solving the inequality $\max\{3 - \alpha, \frac{9}{2} - 2\alpha\} > 5 - 2\alpha$, we see that the right hand side of (22) should be negative for $N \in \mathbb{N}$ large enough whenever $\alpha > 2$. Consequently, we obtain the following corollary.

Corollary 1. *For any $\alpha > 2$, suppose that $\Delta t := N^{-\alpha}$. Then, for sufficiently large N , $L^{n+1} \leq L^n$ is valid for each $n \geq 0$.*

Remark 3. *In [20], a lot of numerical experiments were carried out with $N = 100$ and $\Delta t := 0.1N^{-2}$. This choice seems to be reasonable since $\Delta t = N^{-\frac{5}{2}}$ and this setting is consistent with the result of Corollary 1.*

4 Numerical examples

4.1 Pi curve

We borrowed the coordinate of the pi curve as an initial data from <https://ja.wolframalpha.com/> as [20]. See Figure 1 for a numerical result.

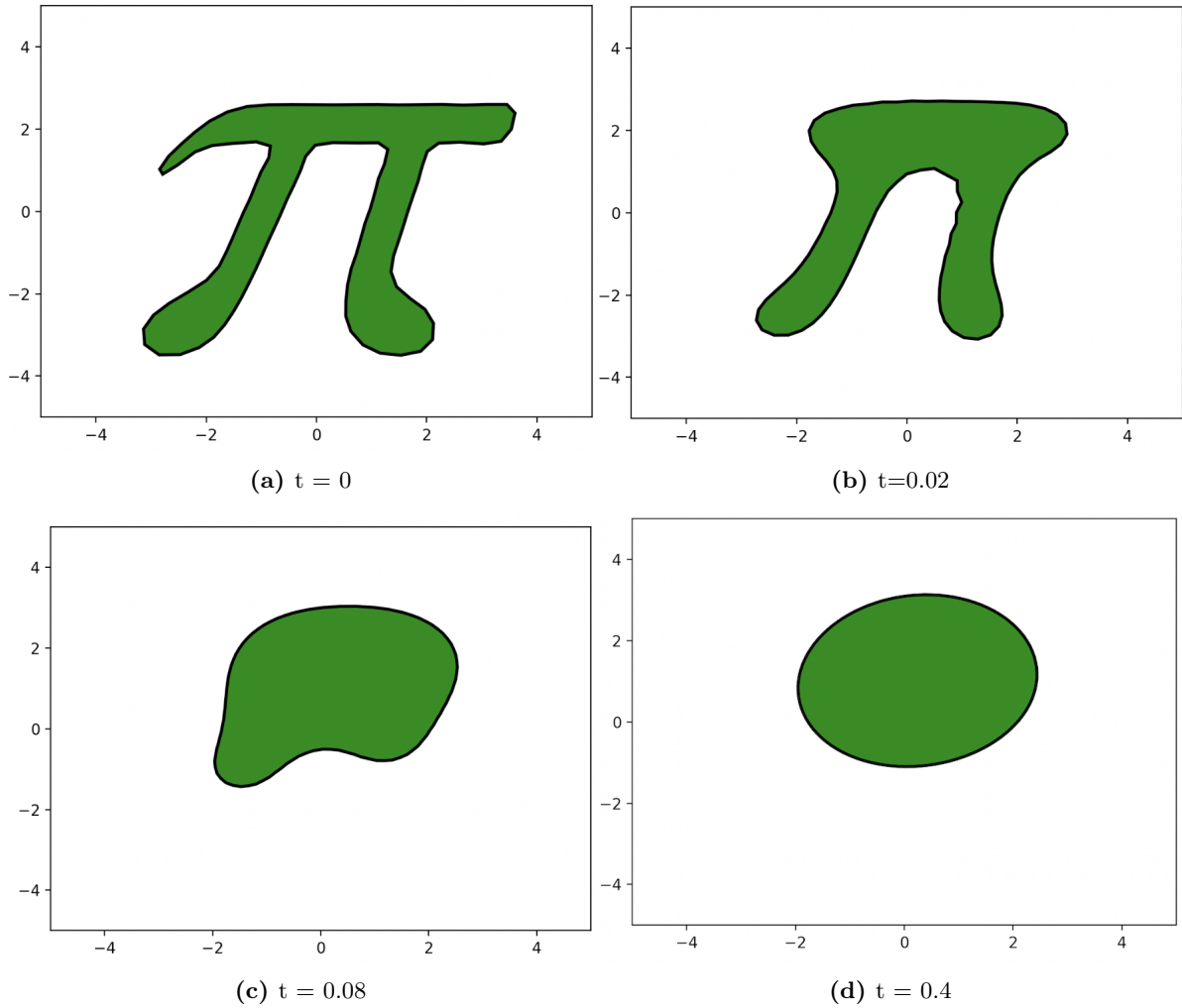


Figure 1: Evolution of Pi shaped curve. $N = 100, \Delta t = 0.1N^{-2}$.

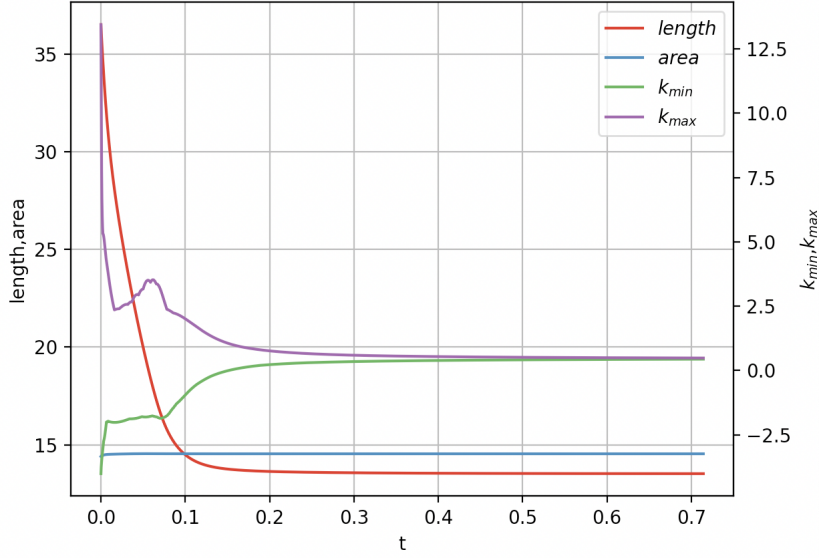


Figure 2: Time evolution of length, area and curvatures for pi-curve.

To confirm uniform boundedness of Q_0^+ , $\frac{1}{N} \sum_{j=1}^N |Q_j^+|$, Q_0^- and $\frac{1}{N} \sum_{j=1}^N |Q_j^-|$ for large N , we extract the first step of the scheme for each N and draw the values of them as a graph. We infer from Figure 3 that all of them may be dominated by some constants and only depend on the initial curve.

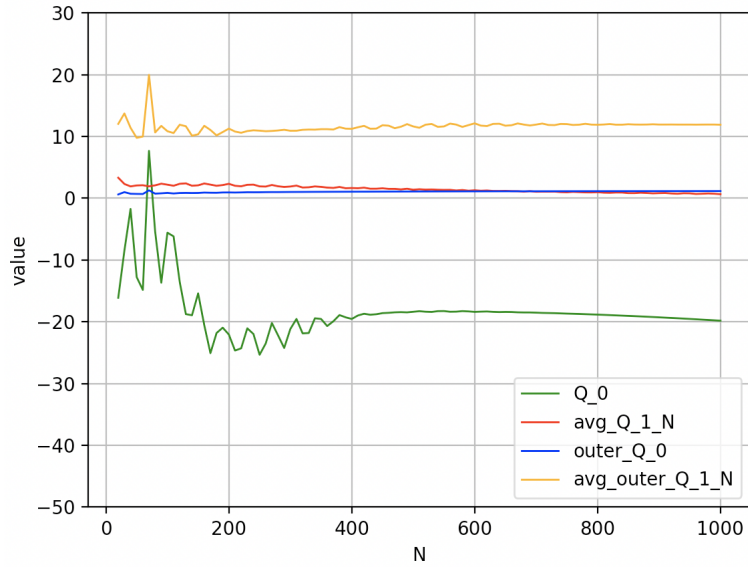


Figure 3: N dependence of coefficients.

4.2 Star

A star shaped curve is somehow close to a circle. As expected, this shape is deformed to a circle by our scheme. See Figure 4 for a numerical result.

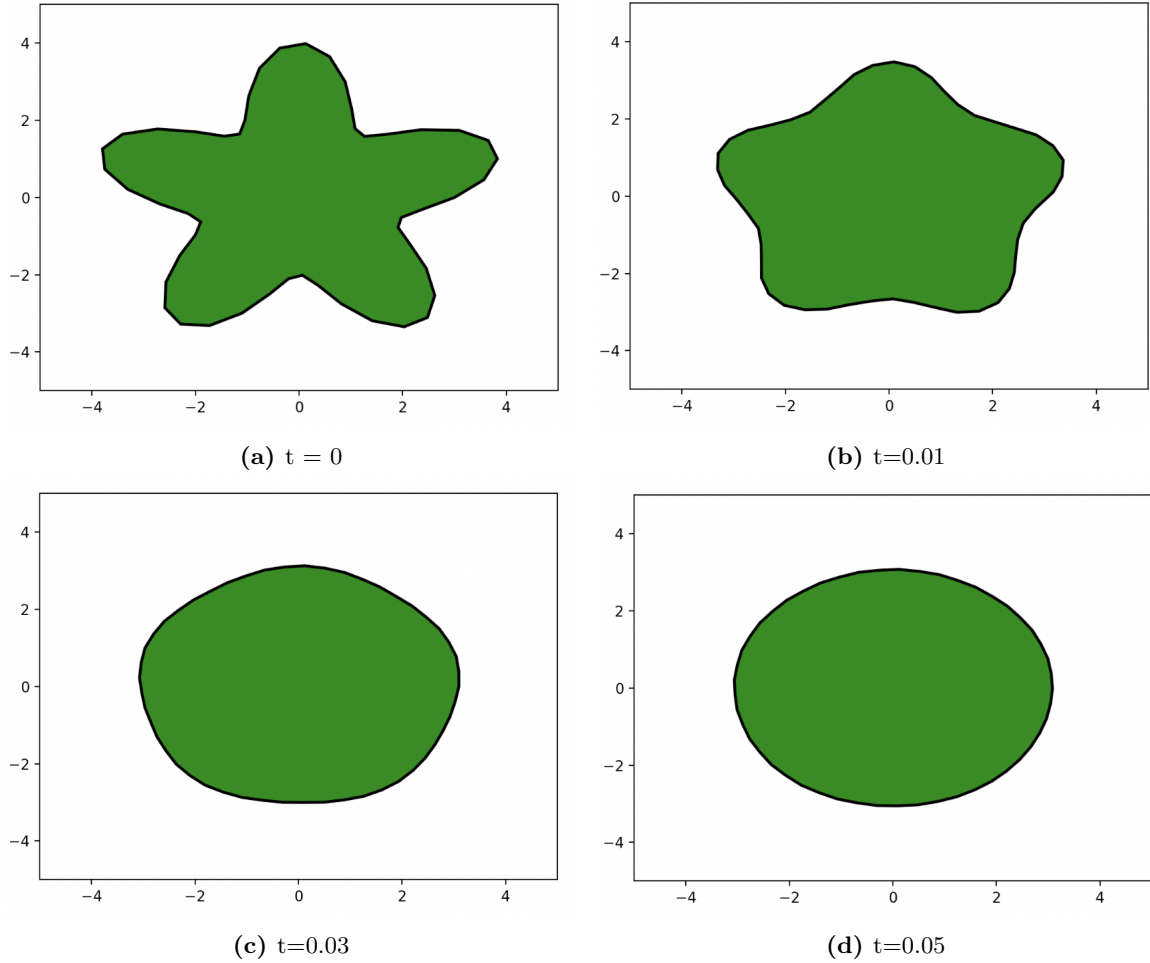


Figure 4: Evolution of Star shaped curve. $N = 50, \Delta t = 0.1N^{-2}$.

4.3 Tube

Mayer [14] showed that the one-sided Mullins-Sekerka flow, that is the Hele-Shaw flow, does not necessarily preserve convexity of an initial curve. This is a unique feature of the Mullins-Sekerka flow. This fact was also numerically observed by Bates et al [4] provided that an initial curve is a tube which has two circular end caps even in the 2-phase Mullins-Sekerka flow. We shall confirm that our scheme yields a same result as well. We set $N = 50, \Delta t = 0.1N^{-2}$. In addition, assume that the length and the thickness of the tube are 8.0 and 1.0, respectively.

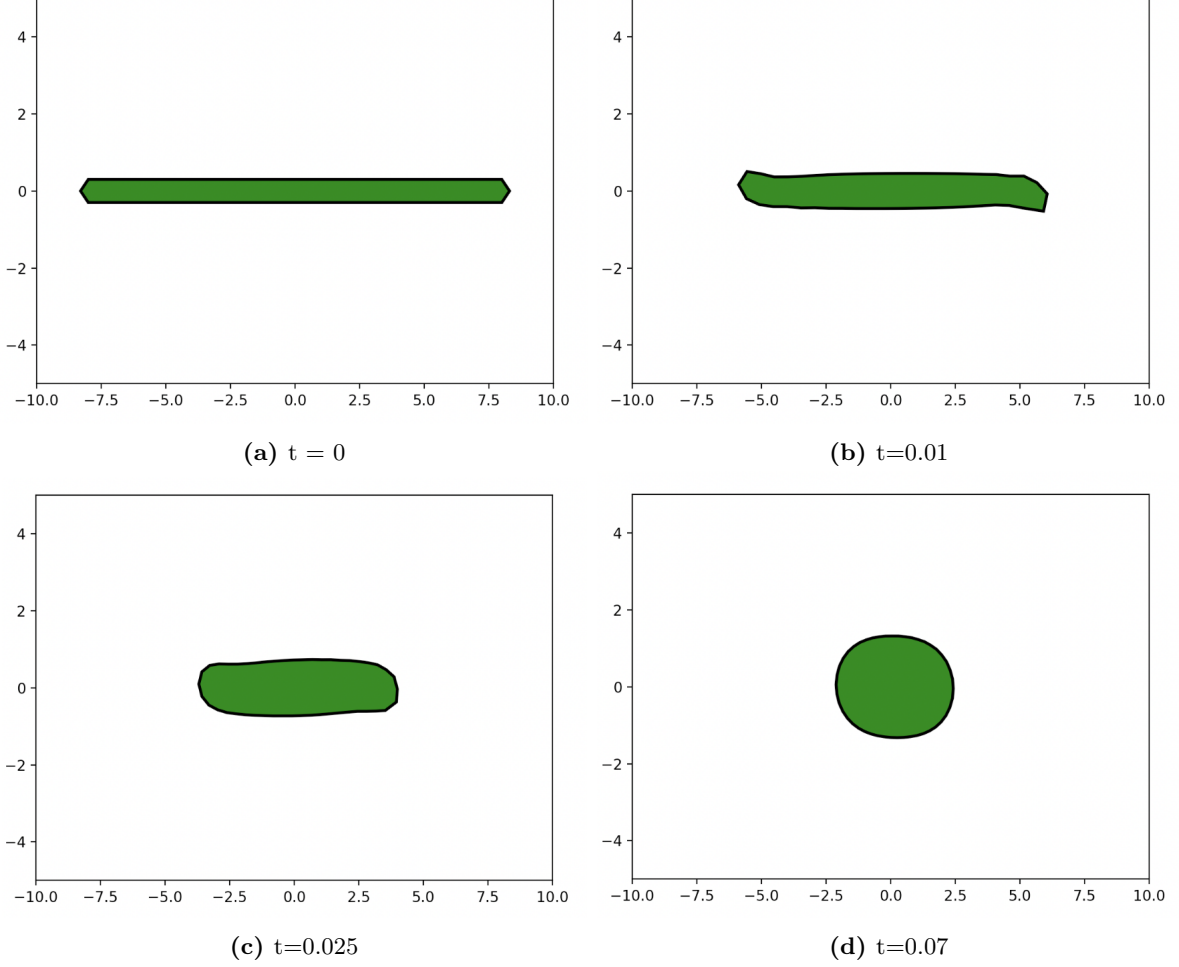


Figure 5: Evolution of Tube shaped curve.

4.4 Accuracy of the scheme

To justify our scheme, we should confirm the accuracy of the scheme. To this end, we need an exact solution of the Mullins-Sekerka problem. Fortunately, it is available in the case where an initial curve is a pair of concentric circles as mentioned in [4]. Let us write below the explicit form of the solution. For $0 < R_1 < R_2$, define u by

$$u(x) := \begin{cases} \frac{1}{R_2} & \text{if } |x| \geq R_2, \\ -\frac{1}{R_1} + \frac{\left(\frac{1}{R_1} + \frac{1}{R_2}\right) \log \frac{|x|}{R_1}}{\log \frac{R_2}{R_1}} & \text{if } R_1 \leq |x| < R_2, \\ -\frac{1}{R_1} & \text{if } |x| < R_1. \end{cases} \quad (23)$$

One can easily observe that the above u is harmonic except on the concentric circles $\partial B_{R_2} \cup \partial B_{R_1}$. The jump of the normal derivatives of u across $\partial B_{R_2} \cup \partial B_{R_1}$ can be explicitly computed as follows. For $x \in \partial B_{R_2}$,

$$\nabla u^i \cdot \mathbf{n} = \frac{x}{|x|^2} \frac{\frac{1}{R_1} + \frac{1}{R_2}}{\log \frac{R_2}{R_1}} \cdot \frac{x}{|x|} = \frac{\frac{1}{R_1} + \frac{1}{R_2}}{R_2 \log \frac{R_2}{R_1}}, \nabla u^e \cdot \mathbf{n} = 0.$$

Thus we have

$$-\left[\frac{\partial u}{\partial \mathbf{n}}\right]_{\partial B_{R_2}} = \nabla u^e \cdot \mathbf{n} - \nabla u^i \cdot \mathbf{n} = -\frac{\frac{1}{R_1} + \frac{1}{R_2}}{R_2 \log \frac{R_2}{R_1}}. \quad (24)$$

Noting that $\Gamma = \overline{B_{R_2}} \setminus B_{R_1}$ and the outer normal vector of Γ on ∂B_{R_1} is equal to $-\frac{x}{|x|}$, it also follows that

$$-\left[\frac{\partial u}{\partial \mathbf{n}}\right]_{\partial B_{R_1}} = \nabla u^e \cdot \mathbf{n} - \nabla u^i \cdot \mathbf{n} = \frac{\frac{1}{R_1} + \frac{1}{R_2}}{R_1 \log \frac{R_2}{R_1}}. \quad (25)$$

The identity (24) implies that the radius of B_{R_2} decreases at the speed $\frac{\frac{1}{R_1} + \frac{1}{R_2}}{R_2 \log \frac{R_2}{R_1}}$. On the other hand, since the outer normal vector field of Γ on ∂B_{R_1} is inward for the ball B_{R_1} , (25) indicates that the radius of B_{R_1} decreases at the speed $\frac{\frac{1}{R_1} + \frac{1}{R_2}}{R_1 \log \frac{R_2}{R_1}}$. Let us compare the radiuses of the concentric circles when our scheme and the above explicit velocity are applied. Since the radiuses $R_1(t)$ and $R_2(t)$ at each time $t \geq 0$ cannot be explicitly computed, we are forced to construct a dummy exact solution by means of a proper discretization with respect to t . In this case, we should remark that the evolution by the Mullins-Sekerka flow eventually corresponds to the one by the Hele-Shaw flow because the normal derivative from the outer domain identically equals zero. In this experiment, we set $R_1 := 1$ and $R_2 := 3$.

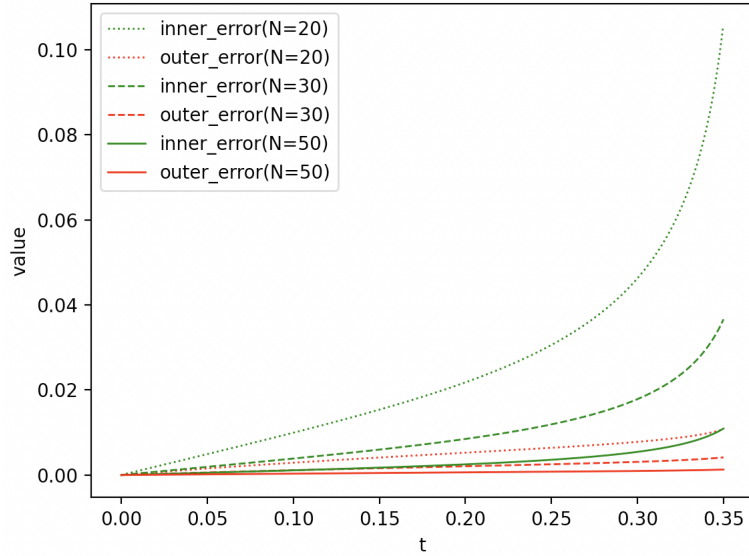


Figure 6: Accuracy check result

Here “inner error” denotes the absolute value of the difference between the accurate radius of the inner circle and the approximate radius derived by our scheme. We present “outer error” in a similar way by means of the outer circle. As shown in Figure 6, the time $t = 0.35$ is a brow up time of the scheme which is consistent to the result of [4].

4.5 Disappearance of particles

Bates et al. [4] treated the case where there are several particles in \mathbb{R}^2 . According to [4], if particles are disjoint circles, then the largest circle grows and smaller ones shrink and eventually disappear. See Figure 5 [10] for the 3D case. Our scheme can also apply to such a case. In order to observe this phenomenon, we prepare four circles in \mathbb{R}^2 imitated by regular 20-polygons, namely we set $N = 20 * 4 = 80$. While evolving, circles will be removed from the target of the numerical calculation when its area become smaller than a prescribed setting.

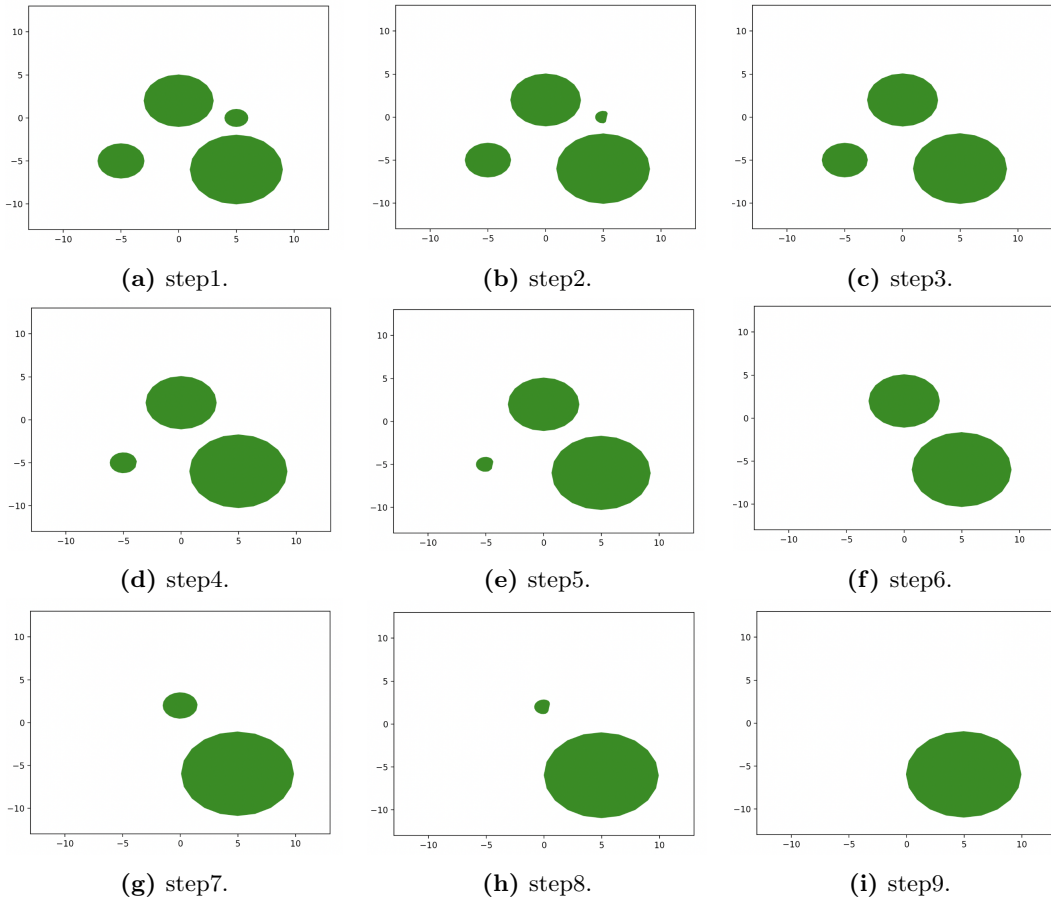


Figure 7: Evolution of multi particles.

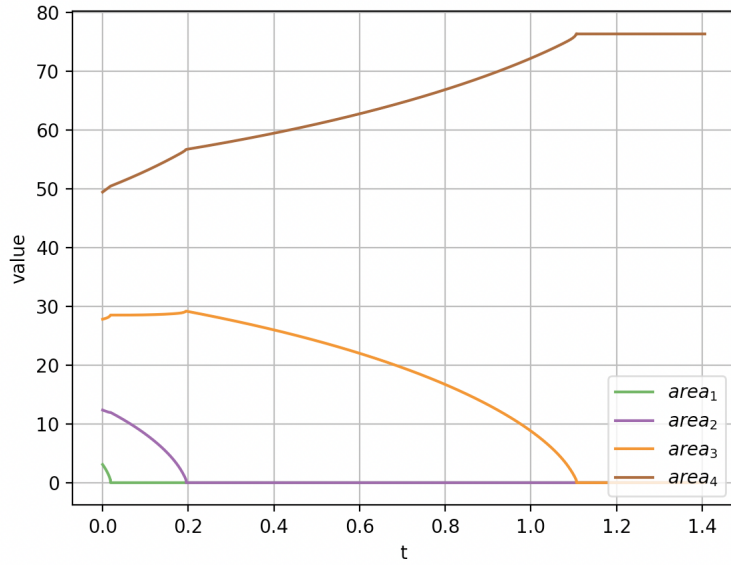


Figure 8: Evolution of areas of each particle

4.6 Coalescence of particles

Setting initial datum as two ovals and putting them closely, we can observe coalescence of particles as shown in Figure 8 [4]. This type of phenomenon was rigorously formulated by Röger [19] with the aid of the notion of varifolds. He was successful to establish the existence of a weak solution of the Mullins-Sekerka problem without the assumption that the loss of area never happens. However, there is no uniqueness result of the weak solution. In this experiment, we check the distance between collocation points of the ovals step by step. If the distance becomes lower than a prescribed value, then we remove the collocation points and its neighbor collocation points from the ovals. Secondly, we artificially connect the ovals and regard them as one polygon. Each oval has 42 collocation points, that is $N = 42 * 2 = 84$. For the numerical result, see Figure 9.

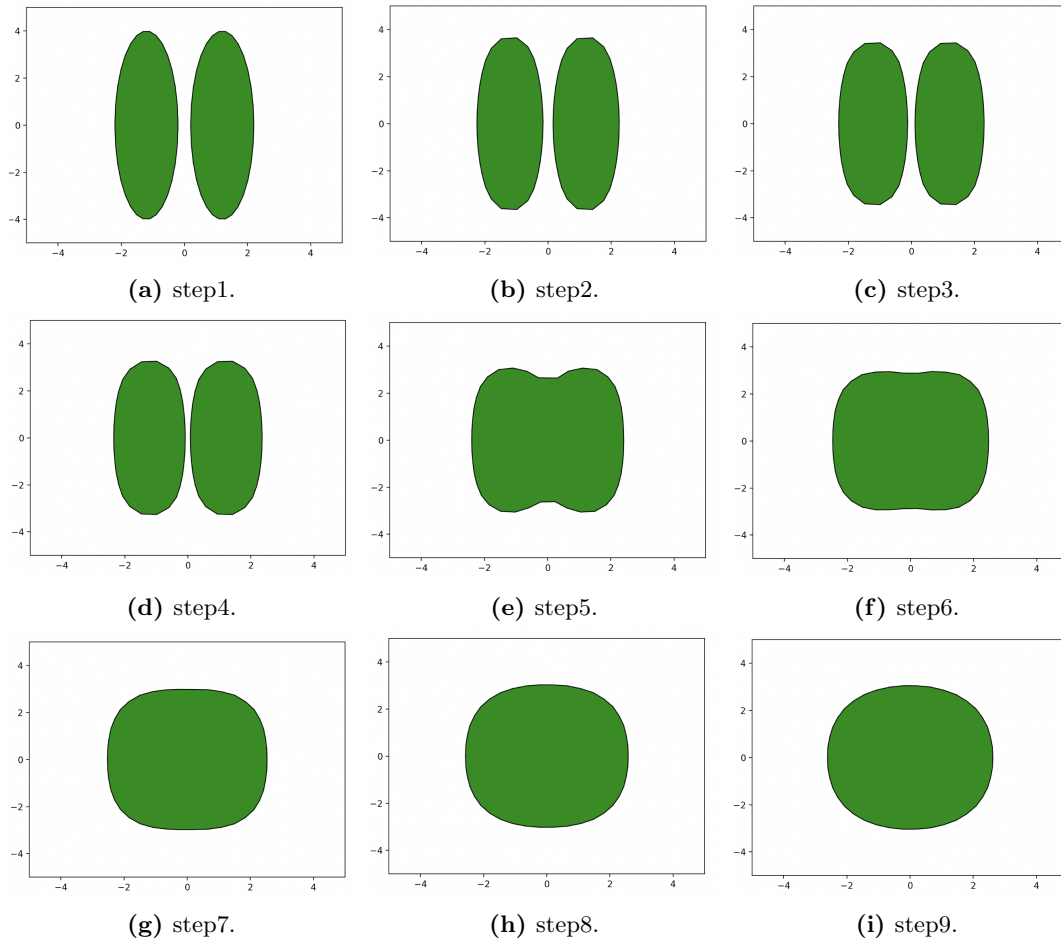


Figure 9: Coalescence of particles.

4.7 Dumbbell

When the initial data is a dumbbell that is the sum set of two circles connected by a narrow bar, a pinch off phenomenon may occur. For example, let r, l and b be the radius of circle, the length of the bar and the thickness of the bar, respectively and set $r := 30, l := 5, b := 0.25$. Then the thickness of the dumbbell decreases in time and eventually pinches off. In this case, we remove the vertices of the polygon when the thickness of the bar becomes smaller than a prescribed value. See Figure 10.

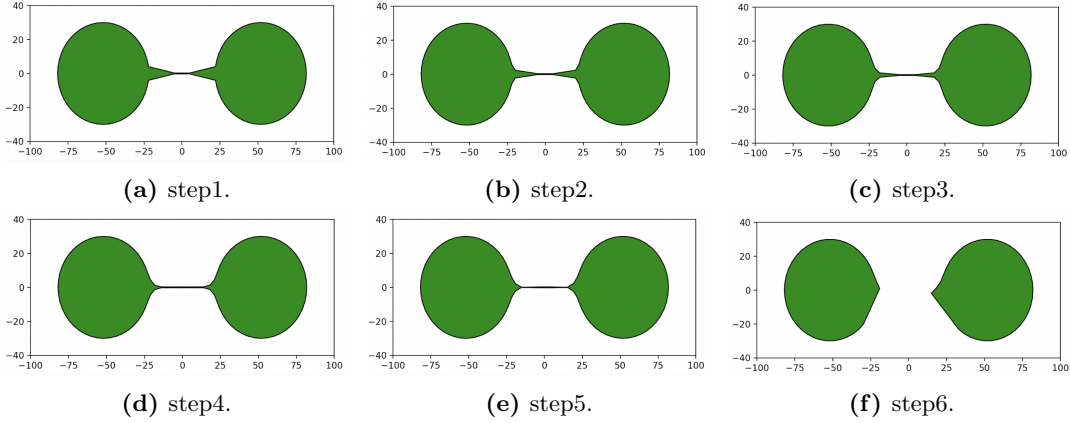


Figure 10: Pinch off of a dumbbell.

To avoid this phenomenon, we may adopt more general form of the Mullins-Sekerka equation, that is to say, we consider the following problem instead of (1).

$$\begin{cases} \Delta u = 0 & \text{in } \mathbb{R}^2 \setminus \Gamma_t, \\ u = \kappa & \text{on } \Gamma_t, \\ \nabla u = O\left(\frac{1}{|x|^2}\right) & \text{as } |x| \rightarrow \infty, \\ V = \sigma_e \frac{\partial u^e}{\partial \mathbf{n}} - \sigma_i \frac{\partial u^i}{\partial \mathbf{n}} & \text{on } \Gamma_t. \end{cases} \quad (26)$$

Here σ_e and σ_i are positive constants that are generally different. These quantity designate the heat diffusion efficiency of the two phases. Observe that the area \mathfrak{A}_t is conserved and the length \mathfrak{L}_t is decreasing in time even if $\sigma_e \neq \sigma_i$. For this type of the presentation of the Mullins-Sekerka equation, see P.558 [18] for instance. Now set $\sigma_e := 1000, \sigma_i := 1$ to prevent the dumbbell from pinching off. See Figure 11.

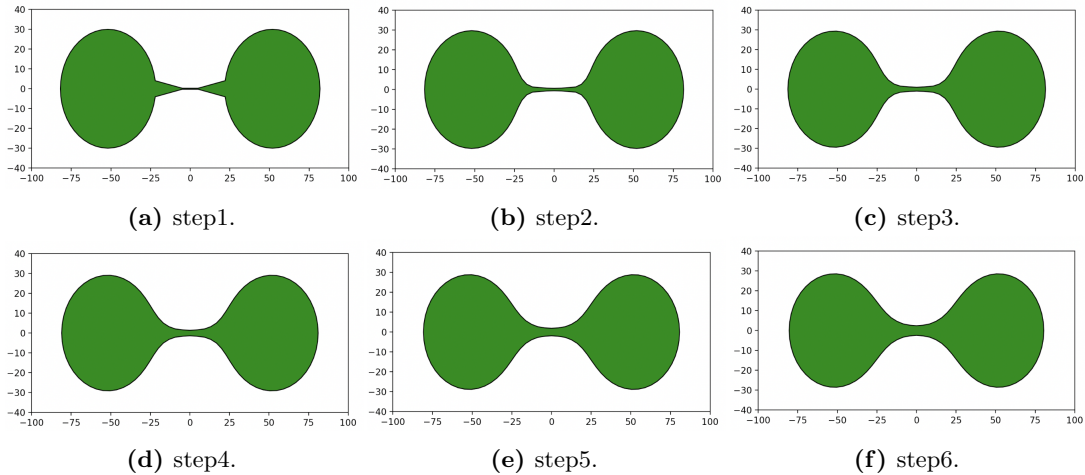


Figure 11: Dumbbell does not pinch off.

5 Extension to boundary contact cases

Let us consider the Mullins-Sekerka flow with the homogeneous Neumann boundary condition in the half plane $\mathbb{R}_+^2 := \{(x_1, x_2) \in \mathbb{R}^2 | x_2 > 0\}$. Formally, a problem we are concerned with is written as follows.

$$\begin{cases} \Delta u = 0 & \text{in } \mathbb{R}_+^2, \\ u = \kappa & \text{on } \Gamma_t, \\ \frac{\partial u}{\partial \mathbf{n}} = 0 & \text{on } \partial \mathbb{R}_+^2, \\ \nabla u = O\left(\frac{1}{|x|^2}\right) & \text{as } |x| \rightarrow \infty, \\ V = -\left[\frac{\partial u}{\partial \nu}\right] & \text{on } \Gamma_t. \end{cases} \quad (27)$$

Here Γ_t is an open curve in \mathbb{R}_+^2 whose end points are bonded on $\partial \mathbb{R}_+^2$ for every $t \geq 0$.

Alternative fundamental solutions. To treat this problem numerically, we have to use another type of approximate solutions different from (9) and (11). Let us explain how to construct approximate solutions to (27) step by step. Similarly to the case where Γ_t does not touch the boundary, suppose that Γ_t^N is an N polygon whose vertices are $\mathbf{X}_i (1 \leq i \leq N)$. The indexes are numbered counterclockwise so that \mathbf{X}_1 and \mathbf{X}_N are the end points of Γ_t^N . \mathbf{X}_1 and \mathbf{X}_N are allowed to move in time only on $\partial \mathbb{R}_+^2$, that is the x_1 -axis. The singular points $y_i^\pm, z_i^\pm (2 \leq i \leq N)$ are put as $y_i^\pm := \mathbf{X}_i^* \pm d\mathbf{n}_i, z_i^\pm := 1000 * y_i, z_i^- := \mathbf{X}_i^* - \frac{d}{2}\mathbf{n}_i$. Now we shall define approximate solutions U^+ and U^- as below.

$$U^+(x) := Q_0^+ + \sum_{j=1}^N Q_j^+ \{E(x - y_j^+) - E(x - z_j^+) + E(x - \bar{y}_j^+) - E(x - \bar{z}_j^+)\}, \quad (28)$$

$$U^-(x) := Q_0^- + \sum_{j=1}^N Q_j^- \{E(x - y_j^-) - E(x - z_j^-) + E(x - \bar{y}_j^-) - E(x - \bar{z}_j^-)\} \quad (29)$$

where we have used the notation $\bar{y} := (y', -y_n)$ when $y = (y', y_n) \in \mathbb{R}^{N-1} \times \mathbb{R}$. Observe that the functions U^+ and U^- are symmetric across the x_1 -axis and fulfill the homogeneous Neumann boundary conditions due to their structure. The real numbers $Q_i^\pm (0 \leq i \leq N)$ are determined with the aid of the Dirichlet boundary condition and the AP property. We should note that κ_2 and κ_N are affected by the contact angle between Γ_t^N and $\partial \mathbb{R}_+^2$ which is not originally geometry of Γ_t^N . Thus, we replace the definition of κ_2 and κ_N by

$$\kappa_2 := \frac{2 \tan_2}{r_2}, \quad \kappa_N := \frac{2 \tan_N}{r_N}.$$

Modified normal velocity at the end points. We have allowed the end points \mathbf{X}_1 and \mathbf{X}_N to move in time but bonded them to the x_1 -axis. Thus, it is necessary to modify the normal velocity at these points what we have defined at (13). Suppose that the contact angle between Γ_t^N and the x_1 -axis at \mathbf{X}_1 equals θ . When the edge $[\mathbf{X}_1, \mathbf{X}_2]$ moves with the speed V to the direction of \mathbf{n}_2 , the movement of the end point \mathbf{X}_1 should equal $\frac{V}{\sin \theta}$. Taking into account this observation, let us define new normal velocity vectors at the end points as follows.

$$\dot{\mathbf{X}}_1(t) := \left(\frac{V_1^+ + V_1^-}{\sin(\arccos(\mathbf{t}_1 \cdot \mathbf{e}_1))} \right) \mathbf{e}_1, \quad \dot{\mathbf{X}}_N(t) := \left(\frac{V_N^+ + V_N^-}{\sin(\arccos(\mathbf{t}_N \cdot \mathbf{e}_1))} \right) \mathbf{e}_1.$$

Here we have used the notation that $\mathbf{e}_1 := (1, 0) \in \mathbb{R}^2$.

Modified UDM. We are also forced to change the way to implement the method of uniformly distribution for the vertices \mathbf{X}_i because \mathbf{X}_1 and \mathbf{X}_N never move along with the tangential vector of Γ_t and the edge $[\mathbf{X}_N, \mathbf{X}_1]$ is not included in Γ_t^N . Tangential velocity $W_i (1 \leq i \leq N)$ are required to satisfy the following linear system.

$$\begin{cases} L = \sum_{i=2}^N r_i, \quad \dot{L} = \sum_{i=2}^N \kappa_i v_i r_i, \\ -\cos_i W_i + \cos_{i+1} W_{i+1} = \frac{\dot{L}}{N-1} + \left(\frac{L}{N-1} - r_i \right) \omega - V_{i+1} \sin_{i+1} - V_i \sin_i \quad \text{for } 2 \leq i \leq N, \\ W_1 = W_N = 0. \end{cases}$$

By these changes from the case where Γ_t is a simply closed curve, we can determine velocity vectors $\dot{\mathbf{X}}_i$ for each $1 \leq i \leq N$. We shall exhibit a numerical result of a simulation for the Mullins-Sekerka flow by means of the way proposed above. An initial open curve is an L-shaped and contacts to the x_1 -axis with the ninety degree angle at two end points. The collocation points are equi-placed and are put at least the corners of the character L. Though the contact angles become different from the ninety degree as soon as we start the program, they eventually converge to the ninety degree and the shape of the curve tend to a semicircle in finite time.

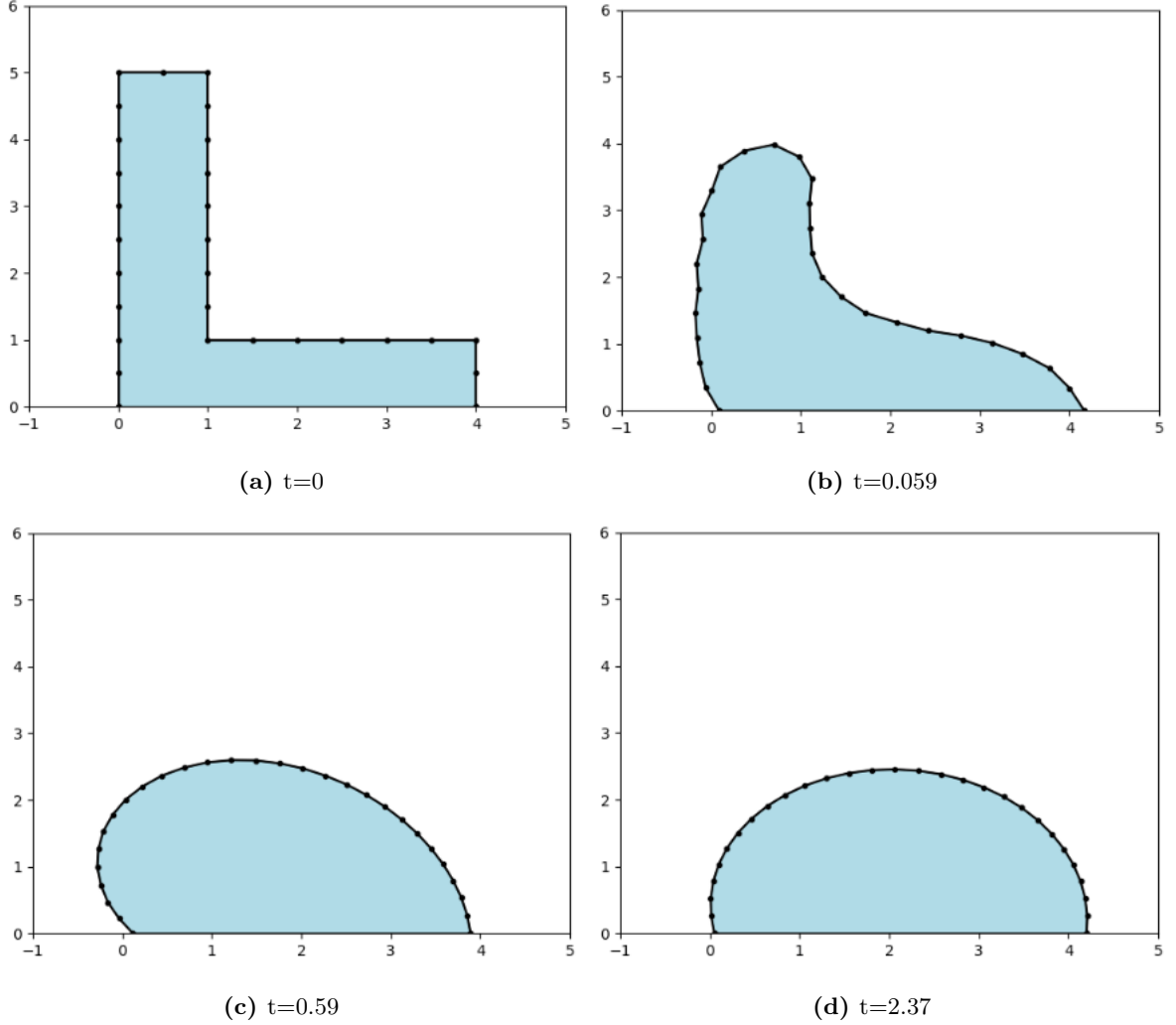


Figure 12: Evolution of L-shaped open curve.

Remark 4. As mentioned in Section 1, local well-posedness of the problem (27) has been shown in [1] whenever Γ_t is perpendicular to the boundary $\partial\mathbb{R}_+^2$, that is to say, $\angle(\Gamma_t, \partial\mathbb{R}_+^2) = \frac{\pi}{2}$. We should note that our scheme yields contact angles not being equal to $\frac{\pi}{2}$ and this result is different from [1]. This outcome implies that there might be a solution to (27) with a general contact angle condition.

6 Acknowledgements

The author has learned the way to express curves on the plane and background of the method of fundamental solutions from Yazaki's monograph. The author is grateful to professor Norikazu Saito for his suggestion to apply the charge simulation method to this problem. He reviewed the manuscript and gave me a lot of helpful comments to brush up the paper. Professor Yoshikazu Giga encouraged the author to consider the case where the heat diffusion

coefficients are different and examine it.

7 Sequence of the proofs

In this section, we list proofs of the results presented in Section 3 that have been postponed.

Lemma 1. *Let the initial curve Γ_0 be a Jordan curve in \mathbb{R}^2 having at least C^2 -regularity. Assume that dummy singular points z_i are taken as $z_i = \frac{d}{2}\mathbf{n}_i$ and collocation points \mathbf{X}_i are equi-placed, that is to say $r_i = \frac{L}{N}$. Then, for each $1 \leq i, j \leq N$,*

$$|G_{i,j}| = O(1), |\mathbf{H}_{i,j}| = O(\sqrt{N}), |H_j| = O(\sqrt{N}) \text{ as } N \rightarrow \infty.$$

Proof. Since Γ does not cross to itself, we can choose N so large that either $|\mathbf{X}_i^* - y_j| \geq |\mathbf{X}_i^* - y_{i+1}|$ or $|\mathbf{X}_i^* - y_j| \geq |\mathbf{X}_i^* - y_{i-1}|$ hold. Assume that the former condition is valid. Fix $1 \leq i, j \leq N$ with $i < j$. Applying the Taylor expansion to $x \mapsto \log|x|$ around $\mathbf{X}_i^* - y_j$ and evaluating at $x = \mathbf{X}_i^* - z_j$ shows

$$\log|\mathbf{X}_i^* - z_j| = \log|\mathbf{X}_i^* - y_j| + \frac{\mathbf{X}_i^* - y_j}{|\mathbf{X}_i^* - y_j|^2} \cdot (y_j - z_j) + O(|y_j - z_j|^2).$$

It readily follows that $|y_j - z_j| = \frac{d}{2} = \frac{1}{2\sqrt{N}} = O(\frac{1}{\sqrt{N}})$. Moreover, viewing the triangle $\triangle \mathbf{X}_i^* y_{i+1} \mathbf{X}_{i+1}^*$, we deduce from the cosine theorem that

$$\begin{aligned} |\mathbf{X}_i^* - y_{i+1}|^2 &= d^2 + r^2 \cos^2 \varphi_i - 2dr \cos \varphi_i \cos \left(\frac{\varphi_i}{2} + \frac{\pi}{2} \right) \\ &= O\left(\frac{1}{N}\right) + O\left(\frac{1}{N^2}\right) + O\left(\frac{1}{N^{\frac{3}{2}}}\right) = O\left(\frac{1}{N}\right). \end{aligned}$$

Hence we see $|\mathbf{X}_i^* - y_{i+1}| = O(\frac{1}{\sqrt{N}})$ as $N \rightarrow \infty$. Combining these estimates gives

$$|G_{i,j}| = \frac{1}{2\pi} \log \frac{|\mathbf{X}_i^* - y_j|}{|\mathbf{X}_i^* - z_j|} \leq \frac{|y_j - z_j|}{|\mathbf{X}_i^* - y_{i+1}|} + O(|y_j - z_j|^2) = O(1) \text{ as } N \rightarrow \infty.$$

We next consider the function $x \mapsto \frac{x}{|x|^2}$ and again utilize the Taylor expansion to obtain

$$\frac{\mathbf{X}_i^* - z_j}{|\mathbf{X}_i^* - z_j|^2} = \frac{\mathbf{X}_i^* - y_j}{|\mathbf{X}_i^* - y_j|^2} + \frac{1}{|\mathbf{X}_i^* - y_j|^2} \left(I - \frac{2(\mathbf{X}_i^* - y_j) \otimes (\mathbf{X}_i^* - y_j)}{|\mathbf{X}_i^* - y_j|^2} \right) (y_j - z_j) + O(|y_j - z_j|^2).$$

Thus we have

$$\begin{aligned} |\mathbf{H}_{i,j}| &= \frac{1}{2\pi} \left| \frac{1}{|\mathbf{X}_i^* - y_j|^2} \left(I - \frac{2(\mathbf{X}_i^* - y_j) \otimes (\mathbf{X}_i^* - y_j)}{|\mathbf{X}_i^* - y_j|^2} \right) (y_j - z_j) + O(|y_j - z_j|^2) \right| \\ &\leq \frac{1}{2\pi} \frac{1}{|\mathbf{X}_i^* - y_{i+1}|^2} \left| I - \frac{2(\mathbf{X}_i^* - y_j) \otimes (\mathbf{X}_i^* - y_j)}{|\mathbf{X}_i^* - y_j|^2} \right|_2 |y_j - z_j| + O(|y_j - z_j|^2) \\ &= O(N) \times O\left(\frac{1}{\sqrt{N}}\right) + O\left(\frac{1}{N}\right) = O(\sqrt{N}) \text{ as } N \rightarrow \infty. \end{aligned}$$

Finally, let us estimate H_j . By the definition,

$$|H_j| = \left| - \sum_{i=1}^N \mathbf{H}_{i,j} \cdot \mathbf{n}_i r_i \right| \leq \sum_{i=1}^N O(\sqrt{N}) \times \frac{L}{N} = O(\sqrt{N}).$$

□

Before we prove main theorems, let us prepare some lemmas.

Lemma 2. For each $1 \leq i \leq N$, let S_i defined by

$$S_i(x) := U^+(x)\nabla U^+(x) \cdot \mathbf{n}_i - U^-(x)\nabla U^-(x) \cdot \mathbf{n}_i.$$

Moreover, suppose that $y_i^\pm = \mathbf{X}_i^* \pm d\mathbf{n}_i, z_i^\pm = \mathbf{X}_i^* \pm \tilde{d}\mathbf{n}_i$ for some $d, \tilde{d} > 0$. Then,

$$\sup_{1 \leq i \leq N} \|\nabla S_i\|_{L^\infty(\Gamma_i)} \leq C$$

holds where

$$C := \frac{2L^2}{\pi^2 d^2} \left(\sum_{j=0}^N |Q_j| \right)^2 \left(1 + \sqrt{3}\pi \log \frac{L + \tilde{d}}{d} \right).$$

Proof. A direct differentiation shows

$$\nabla S_i = \nabla U^+ \nabla U^+ \cdot \mathbf{n}_i + U^+ \nabla^2 U^+ \mathbf{n}_i - \nabla U^- \nabla U^- \cdot \mathbf{n}_i - U^- \nabla^2 U^- \mathbf{n}_i. \quad (30)$$

Here the symbol ∇^2 denotes the Hessian. The first two terms of (30) were already estimated in Lemma 1 and the proof of Theorem 2 at [20]. Since the structure of U^- is same as U^+ , it is easy to see that the same argument works well to estimate the third and the fourth terms. We omit the proof. \square

Lemma 3. Let $f : \mathbb{R}^2 \rightarrow \mathbb{R}$ be partially differentiable and satisfy $\nabla f = O\left(\frac{1}{|x|^\alpha}\right)$ as $|x| \rightarrow \infty$ for some $\alpha > 1$. Then, f is bounded in \mathbb{R}^2 .

Proof. From the assumption for ∇f , there exists $R > 0$ such that for some $C > 0$, it holds

$$|x| \geq R \implies |\nabla f(x)| \leq \frac{C}{|x|^\alpha} \quad \forall x \in \mathbb{R}^2.$$

Fix any $x \in \mathbb{R}^2 \setminus B_R$ and set $x_n := (R + n)\frac{x}{|x|}$ for each $n \in \mathbb{N} \cup \{0\}$. We construct a sequence $\{\tilde{x}_n\}_n$ as follows. Apply Taylor's expansion around x_{n-1} to find $\tilde{x}_n \in (x_{n-1}, x_n)$ for which

$$f(x_n) = f(x_{n-1}) + \nabla f(\tilde{x}_n) \cdot (x_n - x_{n-1})$$

holds. Suppose that $x \in [x_{n_0}, x_{n_0+1}]$ for some $n_0 \in \mathbb{N} \cup \{0\}$. Note that $|x_n - x_{n-1}| = 1$ and $|\nabla f(\tilde{x}_k)| \leq \frac{C}{(k-1+R)^\alpha}$ are valid from the construction of $\{x_n\}_n$ and $\{\tilde{x}_n\}_n$. Moreover, we again use Taylor's expansion around $x = x_{n_0}$ to obtain $\tilde{x} \in (x_{n_0}, x)$ such that $f(x) = f(x_{n_0}) + \nabla f(\tilde{x}) \cdot (x - x_{n_0})$. Then, we compute

$$\begin{aligned} |f(x)| &\leq |f(x) - f(x_0)| + |f(x_0)| \\ &\leq |f(x) - f(x_{n_0})| + \sum_{k=1}^{n_0} |f(x_k) - f(x_{k-1})| + |f(x_0)| \\ &\leq \frac{C}{(n_0 + R)^\alpha} + \sum_{k=1}^{n_0} |\nabla f(\tilde{x}_k)| |x_k - x_{k-1}| + |f(x_0)| \\ &\leq \sum_{k=0}^{n_0} \frac{C}{(k + R)^\alpha} + \max_{\overline{B_R}} |f| \leq \sum_{k=0}^{\infty} \frac{C}{(k + R)^\alpha} + \max_{\overline{B_R}} |f|. \end{aligned}$$

Note that the right hand side of the above inequality is finite and is independent on the choice of $x \in \mathbb{R}^2 \setminus B_R$. Therefore, we can conclude that f is bounded in \mathbb{R}^2 . \square

Lemma 4. *The approximate solution U^- defined by (11) satisfies $\nabla U^-(x) = O\left(\frac{1}{|x|^2}\right)$ as $|x| \rightarrow \infty$. Moreover, U^- is bounded in $\mathbb{R}^2 \setminus \Omega$.*

Proof. The first assertion is straightforward from the following calculation.

$$\nabla U^-(x) = \sum_{i=1}^N Q_i^- (\nabla E(x - y_i) - \nabla E(x - z_i)) = \sum_{i=1}^N Q_i^- \left(\frac{x - y_i}{|x - y_i|^2} - \frac{x - z_i}{|x - z_i|^2} \right) \quad (31)$$

$$= \sum_{i=1}^N Q_i^- \left(\frac{x - y_i}{|x - y_i|^2} - \frac{x}{|x|^2} - \frac{x - z_i}{|x - z_i|^2} + \frac{x}{|x|^2} \right) \quad (32)$$

$$= \sum_{i=1}^N Q_i^- \left(\frac{|x|^2 - |x - y_i|^2}{|x - y_i|^2 |x|^2} x - \frac{y_i}{|x - y_i|^2} + \frac{|x - z_i|^2 - |x|^2}{|x - z_i|^2 |x|^2} x + \frac{z_i}{|x - z_i|^2} \right) \quad (33)$$

$$= O\left(\frac{1}{|x|^2}\right) \text{ as } |x| \rightarrow \infty. \quad (34)$$

The second assertion also follows immediately by setting $\alpha := 2$ in Lemma 3. \square

Remark 5. *A similar argument like (32) can be found in [4] in which the boundary integral method was applied to construct an approximate solution of (1). To show decay of the derivative of solutions as $|x| \rightarrow \infty$, they used the area preserving restriction, namely the mean value of the jump of normal derivatives across the phase interface equals zero. Due to the definition (11), we do not have to use the second equality of (12).*

Proof of Theorem 1. Take N so large that \mathbb{A}_N is regular. To confirm that the first value is finite, let us estimate $\det \mathbb{A}_N$ and $\tilde{\mathbb{A}}_N$ separately. The co-factor expansion of \mathbb{A}_N and Lemma 1 gives

$$\begin{aligned} \det \mathbb{A}_N &= \sum_{i=1}^N (-1)^{i+1} \sum_{\sigma \in S(N)} (-1)^{t_\sigma} H_{\sigma(i)} G_{1,\sigma(1)} \cdots G_{i-1,\sigma(i-1)} G_{i+1,\sigma(i+1)} \cdots G_{N,\sigma(N)} \\ &= \sum_{i=1}^N \sum_{\sigma \in S(N)} O(\sqrt{N}) = O(N! N^{\frac{3}{2}}). \end{aligned}$$

Here we should note that $\sharp S(N) = N!$ to get the last order. On the other hand, co-factors of \mathbb{A}_N can be estimated as follows.

$$(\tilde{\mathbb{A}}_N)_{1,1}^T = (-1)^{1+1} \det \mathbb{G} = O(N!).$$

For $2 \leq j \leq N + 1$,

$$(\tilde{\mathbb{A}}_N)_{1,j}^T = (-1)^{1+j} \begin{vmatrix} 1 & G_{1,1} & \cdots & G_{1,j-2} & G_{1,j} & \cdots & G_{1,N} \\ \vdots & & & & & & \\ 1 & G_{N,1} & \cdots & G_{N,j-2} & G_{N,j} & \cdots & G_{N,N} \end{vmatrix} = O(N!).$$

For $2 \leq i, j \leq N + 1$,

$$(\tilde{\mathbb{A}}_N)^T_{i,j} = (-1)^{i+j} \begin{vmatrix} 0 & H_1 & \cdots & H_{j-2} & H_j & \cdots & H_N \\ 1 & G_{1,1} & \cdots & G_{1,j-2} & G_{1,j} & \cdots & G_{1,N} \\ \vdots & \vdots & \ddots & \vdots & \vdots & \ddots & \vdots \\ 1 & G_{i-1,1} & \cdots & G_{i-2,j-2} & G_{i-2,j} & \cdots & G_{i-2,N} \\ 1 & G_{i+1,1} & \cdots & G_{i,j-2} & G_{i,j} & \cdots & G_{i,N} \\ \vdots & \vdots & \ddots & \vdots & \vdots & \ddots & \vdots \\ 1 & G_{N,1} & \cdots & G_{N,j-2} & G_{N,j} & \cdots & G_{N,N} \end{vmatrix} = O(N!\sqrt{N}).$$

By these estimations tell us that while the absolute sum of first columns has the order $O(N!N)$, that of second columns and beyond have the order $O(N!N^{\frac{3}{2}})$. This implies nothing but $\|\tilde{\mathbb{A}}_N\|_1 = O(N!N^{\frac{3}{2}})$. Therefore, we finish the proof of the first value by

$$\|\mathbb{A}_N^{-1}\|_1 = \left\| \frac{1}{\det \mathbb{A}_N} \tilde{\mathbb{A}}_N \right\|_1 = \frac{O(N!N^{\frac{3}{2}})}{O(N!N^{\frac{3}{2}})} \times O(N) = O(N).$$

Recalling the relationship $\mathbf{A}_N \mathbf{Q}_N = \mathbf{K}_N$, we have $\mathbf{Q}_N = \mathbb{A}^{-1} \mathbf{K}_N$. Since Γ is smooth, the curvature on Γ has a global maximum so that $\kappa_i = O(1)$ as $N \rightarrow \infty$ for each $1 \leq i \leq N$. Then, we compute for each $0 \leq i \leq N$,

$$Q_i = \sum_{j=1}^{N+1} (\mathbb{A}_N^{-1})_{i,j} \kappa_{j-1} = \sum_{j=1}^{N+1} \frac{1}{\det \mathbb{A}_N} (\tilde{\mathbb{A}}_N)_{i,j} \kappa_{j-1} = \sum_{j=1}^{N+1} \frac{O(N!\sqrt{N})}{O(N!N^{\frac{3}{2}})} = O(1).$$

□

Proof of 2. As shown in Proposition 1, the derivative of A with respect to the time variable is written by

$$\dot{A} = \sum_{i=1}^N (v_i^+ + v_i^-) r_i + \text{errA}.$$

Due to UDM, it immediately follows that $\text{errA} = 0$. On the other hand, the second equations of (10) and (12) require that $\sum_{i=1}^N v_i^+ r_i = \sum_{i=1}^N v_i^- r_i = 0$. Therefore, we have $\dot{A} = 0$. □

Lemma 5. For each $1 \leq i \leq N$,

$$\begin{aligned} \mathbf{T}_i &= \cos_i \mathbf{t}_i - \sin_i \mathbf{n}_i = \cos_i \mathbf{t}_{i+1} + \sin_i \mathbf{n}_{i+1}, \\ \mathbf{N}_i &= \cos_i \mathbf{n}_i + \sin_i \mathbf{t}_i = \cos_i \mathbf{n}_{i+1} - \sin_i \mathbf{t}_{i+1}. \end{aligned}$$

Proof. This is easily seen if one note that \mathbf{T}_i is derived by either rotating \mathbf{t}_i with the angle $\frac{\phi_i}{2}$ counterclockwise or rotating \mathbf{t}_{i+1} with the angle $\frac{\phi_i}{2}$ clockwise. The second formula immediately follows by rotating the first formula with the angle $\frac{\pi}{2}$. □

We combine the formula (5) with Lemma 5 to get the following formulae.

Lemma 6.

$$\dot{\mathbf{X}}_i = (V_i^+ \cos_i + V_i^- \cos_i - W_i \sin_i) \mathbf{n}_i + (V_i^+ \sin_i + V_i^- \sin_i + W_i \cos_i) \mathbf{t}_i \quad (35)$$

$$= (V_i^+ \cos_i + V_i^- \cos_i + W_i \sin_i) \mathbf{n}_{i+1} + (-V_i^+ \sin_i - V_i^- \sin_i + W_i \cos_i) \mathbf{t}_{i+1}, \quad (36)$$

$$\dot{\mathbf{X}}_{i-1} = (V_{i-1}^+ \cos_{i-1} + V_{i-1}^- \cos_{i-1} + W_{i-1} \sin_{i-1}) \mathbf{n}_i \quad (37)$$

$$+ (-V_{i-1}^+ \sin_{i-1} - V_{i-1}^- \sin_{i-1} + W_{i-1} \cos_{i-1}) \mathbf{t}_i. \quad (38)$$

Proof. The formula with respect to $\dot{\mathbf{X}}_i$ is straightforward by substituting the formulae in Lemma 5 to (5). One with respect to $\dot{\mathbf{X}}_{i-1}$ is obtained by replacing i with $i-1$ in (36). \square

We are now in the position to prove the results stated in Section 3.

Proof of Proposition 1. At first, note that

$$\dot{r}_i = \frac{\mathbf{X}_i - \mathbf{X}_{i-1}}{|\mathbf{X}_i - \mathbf{X}_{i-1}|} \cdot (\dot{\mathbf{X}}_i - \dot{\mathbf{X}}_{i-1}) = \mathbf{t}_i \cdot (\dot{\mathbf{X}}_i - \dot{\mathbf{X}}_{i-1}).$$

Then, we can calculate as follows.

$$\dot{L} = \sum_{i=1}^N \dot{r}_i = \sum_{i=1}^N \mathbf{t}_i \cdot (\dot{\mathbf{X}}_i - \dot{\mathbf{X}}_{i-1}) = \sum_{i=1}^N (\mathbf{t}_i - \mathbf{t}_{i+1}) \cdot \dot{\mathbf{X}}_i \quad (39)$$

$$= \sum_{i=1}^N \{(V_i^+ \sin_i + V_i^- \sin_i + W_i \cos_i) - (-V_i^+ \sin_i - V_i^- \sin_i + W_i \cos_i)\} \quad (40)$$

$$= \sum_{i=1}^N 2(V_i^+ + V_i^-) \sin_i = \sum_{i=1}^N 2 \cdot \frac{v_i^+ + v_{i+1}^+ + v_i^- + v_{i+1}^-}{2 \cos_i} \cdot \sin_i \quad (41)$$

$$= \sum_{i=1}^N (v_i^+ + v_{i+1}^+ + v_i^- + v_{i+1}^-) \tan_i = \sum_{i=1}^N (v_i^+ + v_i^-) (\tan_i + \tan_{i-1}) \quad (42)$$

$$= \sum_{i=1}^N \frac{\tan_i + \tan_{i-1}}{r_i} (v_i^+ + v_i^-) r_i = \sum_{i=1}^N \kappa_i (v_i^+ + v_i^-) r_i. \quad (43)$$

Here, to get (40), we have used (35) and (36). We next confirm (20). We deduce

$$\dot{A} = \sum_{i=1}^N \frac{r_i \mathbf{n}_i + r_{i+1} \mathbf{n}_{i+1}}{2} \cdot \dot{\mathbf{X}}_i \quad (44)$$

$$= \sum_{i=1}^N \left(\frac{r_i}{2} (V_i^+ \cos_i + V_i^- \cos_i - W_i \sin_i) + \frac{r_{i+1}}{2} (V_i^+ \cos_i + V_i^- \cos_i + W_i \sin_i) \right) \quad (45)$$

$$= \sum_{i=1}^N \left(\frac{r_i + r_{i+1}}{2} (V_i^+ + V_i^-) \cos_i + W_i \sin_i \frac{r_{i+1} - r_i}{2} \right) \quad (46)$$

$$= \sum_{i=1}^N \left(\frac{(r_i + r_{i+1})(v_i^+ + v_{i+1}^+ + v_i^- + v_{i+1}^-)}{4} + W_i \sin_i \frac{r_{i+1} - r_i}{2} \right) \quad (47)$$

$$= \sum_{i=1}^N \left(r_i (v_i^+ + v_i^-) - \frac{(r_{i+1} - r_i)(v_{i+1}^+ + v_{i+1}^- - v_i^+ - v_i^-)}{4} + W_i \sin_i \frac{r_{i+1} - r_i}{2} \right) \quad (48)$$

$$= \sum_{i=1}^N r_i (v_i^+ + v_i^-) + \text{errA}. \quad (49)$$

We gain use (35) and (36) to obtain (45). \square

Proof of Theorem 1. We follow the proof of Theorem 2 [20]. Considering the function $\mu \mapsto S_i((1 - \mu)x_i^* + \mu x)$, for each $x \in \Gamma_i$, we have

$$|S_i(x) - S_i(x_i^*)| \leq \int_0^1 |\nabla S_i((1 - \mu)x_i^* + \mu x)| d\mu \cdot |x - x_i^*| \leq \|\nabla S_i\|_{L^\infty(\Gamma_i)} \cdot \frac{L}{2N}. \quad (50)$$

Take $R > 0$ so large that $\Omega \subset\subset B_R$. Then, we get

$$\int_{\Omega} |\nabla U^+|^2 dx + \int_{B_R \setminus \bar{\Omega}} |\nabla U^-|^2 dx \quad (51)$$

$$= \sum_{i=1}^N \left(\int_{\Gamma_i} U^+ \nabla U^+ \cdot \mathbf{n}_i dS - \int_{\Gamma_i} U^- \nabla U^- \cdot \mathbf{n}_i dS \right) + \int_{\partial B_R} U^- \nabla U^- \cdot \mathbf{n} dS \quad (52)$$

$$= \sum_{i=1}^N \int_{\Gamma_i} S_i(x) dS + \int_{\partial B_R} U^- \nabla U^- \cdot \mathbf{n} dS. \quad (53)$$

Here \mathbf{n} denotes the outer unit normal vector field on ∂B_R . On the other hand, we have

$$\dot{L} = \sum_{i=1}^N \kappa_i (v_i^+ + v_i^-) r_i = \sum_{i=1}^N \left(\int_{\Gamma_i} \kappa_i v_i^+ dS + \int_{\Gamma_i} \kappa_i v_i^- dS \right) \quad (54)$$

$$= \sum_{i=1}^N \left(- \int_{\Gamma_i} U^+(\mathbf{X}_i^*) \nabla U^+(\mathbf{X}_i^*) \cdot \mathbf{n}_i dS + \int_{\Gamma_i} U^-(\mathbf{X}_i^*) \nabla U^-(\mathbf{X}_i^*) \cdot \mathbf{n}_i dS \right) \quad (55)$$

$$= - \sum_{i=1}^N \int_{\Gamma_i} S_i(\mathbf{X}_i^*) dS. \quad (56)$$

We shall estimate the integral part on ∂B_R . From Lemma 3, we obtain

$$\left| \int_{\partial B_R} U^- \nabla U^- \cdot \mathbf{n} dS \right| \leq C_N \int_{\partial B_R} dS \cdot O\left(\frac{1}{R^2}\right) = C_N \cdot O\left(\frac{1}{R}\right) \quad \text{as } R \rightarrow \infty. \quad (57)$$

Here we have set $C_N := \sup_{\mathbb{R}^2 \setminus (\Omega \cup \Gamma)} |U^-|$. The identities (53), (56) and the inequality (57), (50) yield

$$\begin{aligned} \dot{L} + \int_{\Omega} |\nabla U^+|^2 dx + \int_{B_R \setminus \bar{\Omega}} |\nabla U^-|^2 dx &= \left| \sum_{i=1}^N \int_{\Gamma_i} (S_i(x) - S_i(\mathbf{X}_i^*)) dS + \int_{\partial B_R} U^- \nabla U^- \cdot \mathbf{n} dS \right| \\ &\leq \sum_{i=1}^N \|\nabla S_i\|_{L^\infty(\Gamma_i)} \cdot \frac{L}{2N} \int_{\Gamma_i} dS + C_N \cdot O\left(\frac{1}{R}\right) \\ &\leq \frac{C}{N} + C_N \cdot O\left(\frac{1}{R}\right) \quad \text{as } R \rightarrow \infty. \end{aligned}$$

Here, $C > 0$ is determined in Lemma 2. Since $d, \tilde{d} = O(\frac{1}{\sqrt{N}})$ and $\sum_{i=0}^N |Q_j| = O(N)$ (See Proposition 2), we derive $C = O(N^3 \log \sqrt{N})$. We have finished the proof. \square

Proof of Theorem 3. First of all, noting that

$$\mathbf{X}_j^{n+1} = \mathbf{X}_j^n + \Delta t (V_j^n \mathbf{N}_j^n + W_j^n \mathbf{T}_j^n)$$

from the construction of the scheme together with the Taylor expansion yield

$$\begin{aligned}
L^{n+1} - L^n &= \sum_{j=1}^N (r_j^{n+1} - r_j^n) = \sum_{j=1}^N (|\mathbf{X}_j^{n+1} - \mathbf{X}_{j-1}^{n+1}| - |\mathbf{X}_j^n - \mathbf{X}_{j-1}^n|) \\
&= \sum_{j=1}^N \left(\frac{\mathbf{X}_j^n - \mathbf{X}_{j-1}^n}{|\mathbf{X}_j^n - \mathbf{X}_{j-1}^n|} \cdot \{\mathbf{X}_j^{n+1} - \mathbf{X}_{j-1}^{n+1} - (\mathbf{X}_j^n - \mathbf{X}_{j-1}^n)\} + O(|\mathbf{X}_j^{n+1} - \mathbf{X}_{j-1}^{n+1} - (\mathbf{X}_j^n - \mathbf{X}_{j-1}^n)|^2) \right) \\
&= \sum_{j=1}^N (\mathbf{t}_j^n \cdot \Delta t (V_j^n \mathbf{N}_j^n + W_j^n \mathbf{T}_j^n - V_{j-1}^n \mathbf{N}_{j-1}^n - W_{j-1}^n \mathbf{T}_{j-1}^n) + \Delta t^2 O(|\mathbf{V}_j^n|^2)) \\
&= \sum_{j=1}^N (\Delta t (V_j^n \sin_j^n + V_{j-1}^n \sin_{j-1}^n + W_j^n \cos_j^n - W_{j-1}^n \cos_{j-1}^n) + \Delta t^2 O(|\mathbf{V}_j^n|^2)).
\end{aligned}$$

Here we have utilized the abbreviation $\mathbf{V}_j^n := V_j^n \mathbf{N}_j^n + W_j^n \mathbf{T}_j^n - V_{j-1}^n \mathbf{N}_{j-1}^n - W_{j-1}^n \mathbf{T}_{j-1}^n$ for short in the remained term of the Taylor expansion. To obtain the fifth equality, one should note that

$$\mathbf{t}_j^n \cdot \mathbf{n}_{j-1}^n = \cos\left(\varphi_j^n - \frac{\pi}{2}\right), \mathbf{t}_j^n \cdot \mathbf{n}_{j-1}^n = \cos\left(\varphi_{j-1}^n + \frac{\pi}{2}\right), \mathbf{t}_j^n \cdot \mathbf{t}_{j+1}^n = \cos \varphi_j^n, \mathbf{t}_j^n \cdot \mathbf{t}_{j-1}^n = \cos \varphi_{j-1}^n.$$

Due to UDM, it is clear that

$$V_j^n \sin_j^n + V_{j-1}^n \sin_{j-1}^n + W_j^n \cos_j^n - W_{j-1}^n \cos_{j-1}^n = \frac{1}{N} \sum_{j=1}^N \kappa_j^n v_j^n r_j^n - \left(r_j^n - \frac{L^n}{N}\right) \cdot 10N \quad (58)$$

for each $1 \leq j \leq N$. Thus, we have

$$\begin{aligned}
L^{n+1} - L^n &= \Delta t \left(\sum_{j=1}^N \kappa_j^n v_j^n r_j^n - 10N \sum_{j=1}^N \left(r_j^n - \frac{L^n}{N}\right) \right) + \Delta t^2 \sum_{j=1}^N O(|\mathbf{V}_j^n|^2) \\
&= \Delta t \cdot \sum_{j=1}^N \kappa_j^n v_j^n r_j^n - 10NL^n + 10NL^n + \Delta t^2 \sum_{j=1}^N O(|\mathbf{V}_j^n|^2) \\
&= \Delta t \cdot \sum_{j=1}^N \kappa_j^n v_j^n r_j^n + \Delta t^2 \sum_{j=1}^N O(|\mathbf{V}_j^n|^2).
\end{aligned}$$

Secondly, it is necessary to estimate the term $O(|\mathbf{V}_j^n|^2)$ by means of N . To this end, recall the way to derive explicit formulae of W_j^n from (14). For each $1 \leq j \leq N$, ψ_j^n can be estimated by

$$\psi_j^n = \frac{1}{N} \sum_{j=1}^N \kappa_j^n v_j^n r_j^n + O(\sqrt{N}) \text{ as } N \rightarrow \infty.$$

Indeed, the definition of ψ_j^n is

$$\psi_j^n := \begin{cases} 0 & \text{if } j = 1, \\ \frac{1}{N} \sum_{j=1}^N \kappa_j^n v_j^n r_j^n - V_{j-1}^n \sin_{j-1}^n - V_j^n \sin_j^n + \left(\frac{L^n}{N} - r_j^n\right) \omega & \text{otherwise.} \end{cases}$$

It is easily seen that $\sin_j^n = O(\frac{1}{N})$ as $N \rightarrow \infty$ from $\sin_j^n \simeq \frac{\varphi_j^n}{2}$ for sufficiently large N and the following observation.

$$O(1) = \hat{\kappa}_j^n = \frac{\varphi_j^n}{\frac{r_j^n + r_{j+1}^n}{2}} = \frac{\varphi_j^n}{O(\frac{1}{N})}.$$

Moreover, we see $V_j^n = O(N^{\frac{3}{2}})$ from Lemma 1 as follows.

$$\begin{aligned} V_j^n &= \frac{v_j^n + v_{j+1}^n}{2 \cos_j^n} = \frac{-\nabla U^+(\bar{\mathbf{X}}_j^n) \cdot \mathbf{n}_j^n - \nabla U^+(\bar{\mathbf{X}}_{j-1}^n) \cdot \mathbf{n}_{j-1}^n}{2 \cos_j^n} \\ &= \frac{-\sum_{j=1}^N \mathbf{H}_j^n \cdot \mathbf{n}_j^n - \sum_{j=1}^N \mathbf{H}_{j-1}^n \cdot \mathbf{n}_{j-1}^n}{2 \cos_j^n} = \sum_{j=1}^N \frac{O(\sqrt{N})}{O(1)} = O(N^{\frac{3}{2}}). \end{aligned}$$

Here we have used a trivial estimate $\cos_j^n = O(1)$ because it tends to zero as $N \rightarrow \infty$. Furthermore, let us obtain the order of the constant C^i that appears in (14) with respect to N . The order of the quantity Ψ_j^i is calculated as

$$\begin{aligned} \sum_{j=1}^N \Psi_j^n &= \sum_{j=1}^N \sum_{k=1}^j \psi_k^n = \sum_{j=1}^N \sum_{k=1}^j \left(\frac{1}{N} \sum_{j=1}^N \kappa_j^n v_j^n r_j^n + O(\sqrt{N}) + O\left(\frac{1}{N}\right) \right) \\ &= \frac{N(N+1)}{2} \left(\frac{1}{N} \sum_{j=1}^N \kappa_j^n v_j^n r_j^n + O(\sqrt{N}) + O\left(\frac{1}{N}\right) \right) = O(N) \sum_{j=1}^N \kappa_j^n v_j^n r_j^n + O(N^{\frac{5}{2}}). \end{aligned}$$

Thus, we get

$$C^n = -\frac{\sum_{j=1}^N \frac{\Psi_j^n}{\cos_j^n}}{\sum_{j=1}^N \frac{1}{\cos_j^n}} = \frac{O(N) \sum_{j=1}^N \kappa_j^n v_j^n r_j^n + O(N^{\frac{5}{2}})}{O(N)} = O(1) \sum_{j=1}^N \kappa_j^n v_j^n r_j^n + O(N^{\frac{3}{2}}).$$

Since Ψ_j^n has lower order than the above quantity, we deduce that

$$W_j^n = \frac{\Psi_j^n + C^n}{\cos_j^n} = O(1) \sum_{j=1}^N \kappa_j^n v_j^n r_j^n + O(N^{\frac{3}{2}}).$$

Let us return to the discussion of the quantity $O(|\mathbf{V}_j^n|^2)$. A direct calculation shows

$$\begin{aligned} |\mathbf{V}_j^n|^2 &= V_j^{n2} + W_j^{n2} + V_{j-1}^{n2} + W_{j-1}^{n2} + 2V_j^n W_j^n \mathbf{N}_j^n \cdot \mathbf{T}_j^n - 2V_j^n V_{j-1}^n \mathbf{N}_j^n \cdot \mathbf{N}_{j-1}^n - 2V_j^n W_{j-1}^n \mathbf{N}_j^n \cdot \mathbf{T}_{j-1}^n \\ &\quad - 2W_j^n V_{j-1}^n \mathbf{T}_j^n \cdot \mathbf{N}_{j-1}^n + 2W_j^n W_{j-1}^n \mathbf{T}_j^n \cdot \mathbf{T}_{j-1}^n + 2V_{j-1}^n W_{j-1}^n \mathbf{N}_{j-1}^n \cdot \mathbf{T}_{j-1}^n \\ &= V_j^{n2} + W_j^{n2} + V_{j-1}^{n2} + W_{j-1}^{n2} - 2V_j^n V_{j-1}^n \cos\left(\frac{\varphi_{j-1}^n + \varphi_j^n}{2}\right) \\ &\quad - 2V_j^n W_{j-1}^n \cos\left(\frac{\varphi_{j-1}^n + \varphi_j^n}{2} - \frac{\pi}{2}\right) - 2W_j^n V_{j-1}^n \cos\left(\frac{\varphi_{j-1}^n + \varphi_j^n}{2} + \frac{\pi}{2}\right) \\ &\quad + 2W_j^n W_{j-1}^n \cos\left(\frac{\varphi_{j-1}^n + \varphi_j^n}{2}\right) \\ &= V_j^{n2} + W_j^{n2} + V_{j-1}^{n2} + W_{j-1}^{n2} - 2V_j^n V_{j-1}^n \cos\left(\frac{\varphi_{j-1}^n + \varphi_j^n}{2}\right) \\ &\quad - 2V_j^n W_{j-1}^n \sin\left(\frac{\varphi_{j-1}^n + \varphi_j^n}{2}\right) + 2W_j^n V_{j-1}^n \sin\left(\frac{\varphi_{j-1}^n + \varphi_j^n}{2}\right) + 2W_j^n W_{j-1}^n \cos\left(\frac{\varphi_{j-1}^n + \varphi_j^n}{2}\right). \end{aligned}$$

Square both side of the identity (58) to get

$$\begin{aligned}
& V_j^{n2} \sin_j^{n2} + V_{j-1}^{n2} \sin_{j-1}^{n2} + W_j^{n2} \cos_j^{n2} + W_{j-1}^{n2} \cos_{j-1}^{n2} \\
& \quad + 2V_j^n V_{j-1}^n \sin_j^n \sin_{j-1}^n + 2V_j^n W_j^n \sin_j^n \cos_j^n - 2V_j^n W_j^n \sin_j^n \cos_{j-1}^n \\
& \quad + 2V_{j-1}^n W_j^n \sin_{j-1}^n \cos_j^n - 2V_{j-1}^n W_{j-1}^n \sin_{j-1}^n \cos_{j-1}^n - 2W_j^n W_{j-1}^n \cos_j^n \cos_{j-1}^n \\
& \qquad \qquad \qquad = \left(\frac{1}{N} \sum_{j=1}^N \kappa_j^n v_j^n r_j^n + O(1) \right)^2. \quad (59)
\end{aligned}$$

Adding a proper quantity to both side of (59) shows that

$$\begin{aligned}
|\mathbf{V}_j^n|^2 &= \left(\frac{1}{N} \sum_{j=1}^N \kappa_j^n v_j^n r_j^n + O(1) \right)^2 + V_j^{n2} \cos_j^{n2} + V_{j-1}^{n2} \cos_{j-1}^{n2} + W_j^{n2} \sin_j^{n2} + W_{j-1}^{n2} \sin_{j-1}^{n2} \\
& \quad - 2V_j^n V_{j-1}^n \cos_j^n \cos_{j-1}^n - 2V_j^n W_{j-1}^n \sin_{j-1}^n \cos_{j-1}^n + 2V_{j-1}^n W_j^n \sin_j^n \cos_{j-1}^n \\
& \quad + 2W_j^n W_{j-1}^n \sin_j^n \sin_{j-1}^n - 2V_j^n W_j^n \sin_j^n \cos_j^n + 2V_{j-1}^n W_{j-1}^n \sin_{j-1}^n \cos_{j-1}^n \\
& \qquad \qquad \qquad = O\left(\frac{1}{N^2}\right) \left(\sum_{j=1}^N \kappa_j^n v_j^n r_j^n \right)^2 + O(\sqrt{N}) \sum_{j=1}^N \kappa_j^n v_j^n r_j^n + O(N^3). \quad (60)
\end{aligned}$$

Summing up through $1 \leq j \leq N$ in (60), we have the desired estimate. \square

References

- [1] H. Abels, R. Maximilian, and M. Wilke. Well-posedness and qualitative behaviour of the mullins-sekerka problem with ninety-degree angle boundary contact. *Math. Ann.*, 381:363–403, 2021.
- [2] N.D. Alikakos, P.W. Bates, and X. Chen. Convergence of the cahn-hilliard equation to the hele-shaw model. *Arch. Rational Mech. Anal.*, 128:165–205, 1994.
- [3] J.W. Barrett, H. Garcke, and R. Nürnberg. On stable parametric finite element methods for the stefan problem and the mullins-sekerka problem with applications to dendritic growth. *J. Comput. Phys.*, 229(18):6270–6299, 2010.
- [4] P. Bates, X. Chen, and X. Deng. A numerical scheme for the two phase mullins-sekerka problem. *Electronic Journal of Differential Equations*, 1995:1–27, 1995.
- [5] P.W. Bates and S. Brouwn. A numerical scheme for the mullins-sekerka evolution in three space dimensions. *Differential equations and computational simulations (Chengdu, 1999)*, page 12–26, 2000.
- [6] X. Chen, J. Hong, and F. Yi. Existence uniqueness and regularity of classical solutions of the mullins—sekerka problem. *Communications in Partial Differential Equations*, 21:11-12:1705–1727, 1996.
- [7] C.L. Epstein and M. Gage. The curve shortening flow, wave motion: Theory, modelling, and computation. *Math. Sci. Res. Inst. Publ., Springer*, 7:15–59, 1987.

- [8] J. Escher and G. Simonett. Classical solutions for hele-shaw models with surface tension. *Adv. Differential Equations*, 2(4):619–642, 1997.
- [9] X. Feng and A. Prohl. Numerical analysis of the cahn-hilliard equation and approximation of the hele-shaw problem. *Interfaces Free Bound.*, 7(1):1–28, 2005.
- [10] H. Garcke. Curvature driven interface evolution. *Jahresbericht der Deutschen Mathematiker-Vereinigung*, 115:63–100, 2013.
- [11] M. Katsurada. A mathematical study of the charge simulation method ii. *J. Fac. Sci., Univ. of Tokyo, Sect. IA*, 36:135–162, 1989.
- [12] M. Katsurada and H. Okamoto. A mathematical study of the charge simulation method i. *J. Fac. Sci., Univ. of Tokyo, Sect. IA*, 35:507–518, 1988.
- [13] S. Luckhaus and T. Struzenhecker. Implicit time discretization for the mean curvature flow equation. *Calculus of Variations and Partial Differential Equations*, 3:253–271, 1995.
- [14] Uwe F. Mayer. One-sided mullins-sekerka flow does not preserve convexity. volume 8, pages 1–7, 1993.
- [15] Uwe F. Mayer. A numerical scheme for moving boundary problems that are gradient flows for the area functional. *European J. Appl. Math.*, 11(1):61–80, 2000.
- [16] K. Murota. Comparison of conventional and "invariant" schemes of fundamental solutions method for annular domains." *Jpn J Ind Appl Math*, 1:61–85, December 1995.
- [17] R.L. Pego. Front migration in the nonlinear cahn-hilliard equation. *Proc. R. Soc. Lond. A*, 422:261–278, 1989.
- [18] J. Prüss and G. Simonett. Moving interfaces and quasilinear parabolic evolution equations. *Birkhäuser*, 2019.
- [19] M. Röger. Existence of weak solutions for the mullins-sekerka flow. *SIAM J. Math. Anal.*, 37:291–301, 2005.
- [20] K. Sakakibara and S. Yazaki. Structure-preserving numerical scheme for the one-phase hele-shaw problems by the method of fundamental solutions. *Computational and Mathematical Methods*, 1(6), November 2019.
- [21] Barbara E. E. Stoth. Convergence of the cahn-hilliard equation to the mullins-sekerka problem in spherical symmetry. *J. Differential Equations*, 125(1):154–183, 1996.
- [22] J. Zhu, X. Chen, and T.Y. Hou. An efficient boundary integral method for the mullins-sekerka problem. *J. Comput. Phys.*, 127(2):246–267, 1996.